We are IntechOpen, the world's leading publisher of Open Access books Built by scientists, for scientists

6,900
Open access books available

185,000
International authors and editors

200M
Downloads

Our authors are among the

154
Countries delivered to

TOP 1%
most cited scientists

12.2%
Contributors from top 500 universities



WEB OF SCIENCE™

Selection of our books indexed in the Book Citation Index in Web of Science™ Core Collection (BKCI)

Interested in publishing with us?
Contact book.department@intechopen.com

Numbers displayed above are based on latest data collected.
For more information visit www.intechopen.com



Chapter 1

Biotechnology Processes for Scalable, Selective Rare Earth Element Recovery

Lynne E. Macaskie, Sayo Moriyama,

Iryna Mikheenko, Sarah Singh and Angela J. Murray

Additional information is available at the end of the chapter

http://dx.doi.org/10.5772/intechopen.68429

Abstract

Biorecovery of rare earth elements (REE) from wastes and ores is achieved by bacteria using biogenic phosphates. One approach uses an enzyme that biomineralises REE phosphate crystals into the extracellular polymeric matrix (EPM). The enzyme, co-localised in the EPM, provides a continuous phosphate feed into biomineralisation. The bacteria can be immobilised in a column, allowing continuous metal removal. Metals biocrystallise at different rates. By choosing suitable conditions and column flow rates selective recovery of REE against uranium and thorium can potentially overcome a bottleneck in recovery of REE from mine tailings and ore leachates co-contaminated with these radionuclides. Another approach to REE recovery first lays down calcium phosphate as hydroxyapatite (Bio-HA) using the enzymatic process. Bio-HA then captures REE, loading REE of up to 84% of the HA-mass. REE^{3+} first localises at the grain boundaries of the small bio-crystallites and then substitutes for Ca^{2+} stoichiometrically within the HA. After REE capture the bio-HA/REE hybrid can be separated magnetically. A wider concept: using a 'priming' deposit of one mineral to facilitate the capture of REEs, has been shown, potentially providing a basis for selective REE recovery which would provide advantages over the > 100 steps currently used in commercial REE refining.

Keywords: bacteria, hydroxyapatite, immobilised biofilm, rare earth recovery, rare earth selectivity

INTECH
open science | open minds

© 2017 The Author(s). Licensee InTech. This chapter is distributed under the terms of the Creative Commons Attribution License (http://creativecommons.org/licenses/by/3.0), which permits unrestricted use, distribution, and reproduction in any medium, provided the original work is properly cited. CC BY

1. Introduction

Rare earth elements (REE), listed as 'critical materials' by the EU, are essential for modern electronics and for meeting global commitments to 'green' technologies, e.g. renewable energy (i.e. wind, solar) and energy efficient vehicles [1]. World REE production has approximately doubled in the last decade; consumption was forecast to reach 210,000 T in 2016 but >95% of global REE supply is from China, causing major geopolitical (e.g. soaring prices, restricted export quotas) and environmental issues. Demand for some REE will outstrip supply, leading to economic concerns about security of supply and an urgent requirement to find alternative sources. REE-bearing environments are ubiquitous but are considered too low-grade to be economically extracted or they may contain toxic and/or radioactive elements, complicating REE processing; more than 100 steps are used in current REE purifications.

Currently, hydrometallurgy processes are used to dissolve, separate and purify REE from ores [1]. A widely used method, saponification, produces more than 20 million tonnes of wastewater annually; the scale of the environmental contamination in China has led to substantial remediation bills ($0.25 billion per year) and a warning from the Chinese Ministry of Environmental Protection for REE producers to clean up emissions or face being closed down [2]. Ore extraction has moved towards bio-mining (i.e. bio-leaching/bio-beneficiation), a potentially more economical, environmental friendly approach [3], but it is often overlooked by industry due to longer extraction times, difficulty in controlling microbial reactions and unsuitable ores/materials. Microorganisms are well known to take up REEs [4–9] and can also control the environmental form, mobility and transport of metals [10]. Hence, harnessing biotechnological methods for REE extraction/recovery could lead to more economically viable, environmental friendly processes. For example while inorganic acids can selectively leach REE from clay materials [11], organic acids (such as produced by microbes) were shown to selectively extract REE from phosphate-minerals (apatite/monazite) [12] and soils [13]. Ligands with carboxyl functional groups (similar to the active groups of organic acids as found on microbial cell surfaces and in extracellular polymeric materials) have been shown to be efficient, reusable, selective leaching/extracting agents [14], which could overcome issues associated with the use of toxic additives and the generation of large waste streams [1]. Reactive minerals (often made biogenically) have remarkable morphologies and/or improved functionality for metal removal [15], for example nano-structured MnOx has 400 times higher uptake than commercial material for the removal of contaminants [16, 17], Hydroxyapatite (HA) made in the presence of organic materials can take up Cu(II) to a ten-fold higher extent than its 'chemical' counterpart [18] and biogenic HA can take up Sr^{2+} from saline solution where its chemical counterpart cannot [19]. Alternatively, bacteria can simply synthesise REE phosphate enzymatically to metal loadings of several-fold higher mass than the biomass itself [20, 21]. The neo-mineral is nanoform (14 nm crystallites) [21, 22] which has implications for onward facile processing; with a much larger surface area than large mineral crystals it would be easier to generate a leachate under benign conditions for easier metal recovery from a resulting concentrate.

The purpose of this review is to highlight developments towards a biotechnological approach to REE recovery from solution and to indicate where future opportunities (and difficulties) may lie in a bio-refinery concept towards cleaner, more efficient REE recovery and processing.

The examples described centre upon the use of biogenic REE phosphates, some of which have particular applications, e.g. as catalysts in the manufacture of butadiene rubber (Nd) [23] and as optically active materials (Eu) [24, 25]. The concept of 'one-pot bio-refining' of new material from waste brings new opportunities for application of combinatorial chemistry and synthetic biology which cannot be achieved by chemistry alone and key bottlenecks to progress in novel REE recovery and processing are highlighted.

2. Biotechnology for recovery of rare earth elements from solution

It is well known that microbial cells have a strong affinity for REEs [4–9]. As well as by simple biosorption bacterial systems can accumulate metals as heavy bio-mineral deposits, e.g. see Macaskie et al. [26]. Metallic ions (e.g. UO_2^{2+}, La^{3+}) can be converted into metal phosphate minerals (HUO_2PO_4, $LaPO_4$) enzymatically. Using a well-documented paradigm system [26] a *Serratia* sp. (strain N14; formerly designated as a *Citrobacter* sp.) can, especially under carbon-restriction, up-regulate an acid phosphatase. The corresponding *phoN* gene, under control of the *phoP*/*phoQ* regulon, is up-regulated in response to various cell stresses. The phosphatase is 'trafficked' to and through the cell surface layers (periplasmic space and outer membrane) and locates in the extracellular polymeric matrix (EPM) [27] which comprises heavily hydrated polysaccharide chains and some lipids derived from cell membrane material [27]. The EPM tethers and supports the phosphatase (**Figure 1A**) and, when supplied with a suitable organic phosphate molecule, the enzyme liberates inorganic phosphate to precipitate with metal ions. This forms nucleation sites. Hence, the EPM scaffolds the growing metal phosphate bio-mineral (**Figure 1B**) that grows with addition of further metal and phosphatase substrate. In the case of a biofilm (**Figure 1C**), heavy mineral deposits eventually coat the cells and hence the biofilm (**Figure 1D**). Importantly, the bacteria do not need to be alive as the enzyme is essentially immobilised; the need for metabolism ceases when the enzyme is made and exported into the EPM. The phosphatase activity is stable and hence heavy mineral deposits are obtained (**Figure 1D**). Bacteria readily grow as biofilms on surfaces, such as reticulated polyurethane foam (**Figure 1E** and **F**) 'tethering' the bio-mineral (**Figure 1G**) against the flow within flow-through columns (**Figure 2**). This approach to metal recovery was initially developed for removal of radionuclides from solution where lanthanides such as La^{3+} and Eu^{3+} form a 'surrogate' for trivalent transuranic elements [20, 28, 29]. Effective, continuous metal removal was reported using La^{3+} using cells entrapped in a gel [20]. La is not a highly valuable REE and hence development of REE bio-recovery technology has more recently focused on the removal of Nd^{3+} and Eu^{3+}.

Early work used a gel-immobilisation system with bacteria grown in batch culture as free cells and then immobilised [20]. Shredded gel was placed into a glass column for use as a continuous filter. Later studies using biofilm-immobilised cells (**Figures 1G** and **2**) used columns comprising eight biofilm-coated polyurethane reticulated foam discs stacked in a glass column [21] with solution pumped upwards (flow rates as required). The solution comprised rare earth ions (REE^{3+}), glycerol 2-phosphate (5 mM; phosphate donor to yield inorganic phosphate for the growing mineral) and citrate buffer (2 mM) to the required pH. Citrate provides a known amount of metal chelation. This is important to compare the recovery of different metals in an identical solution

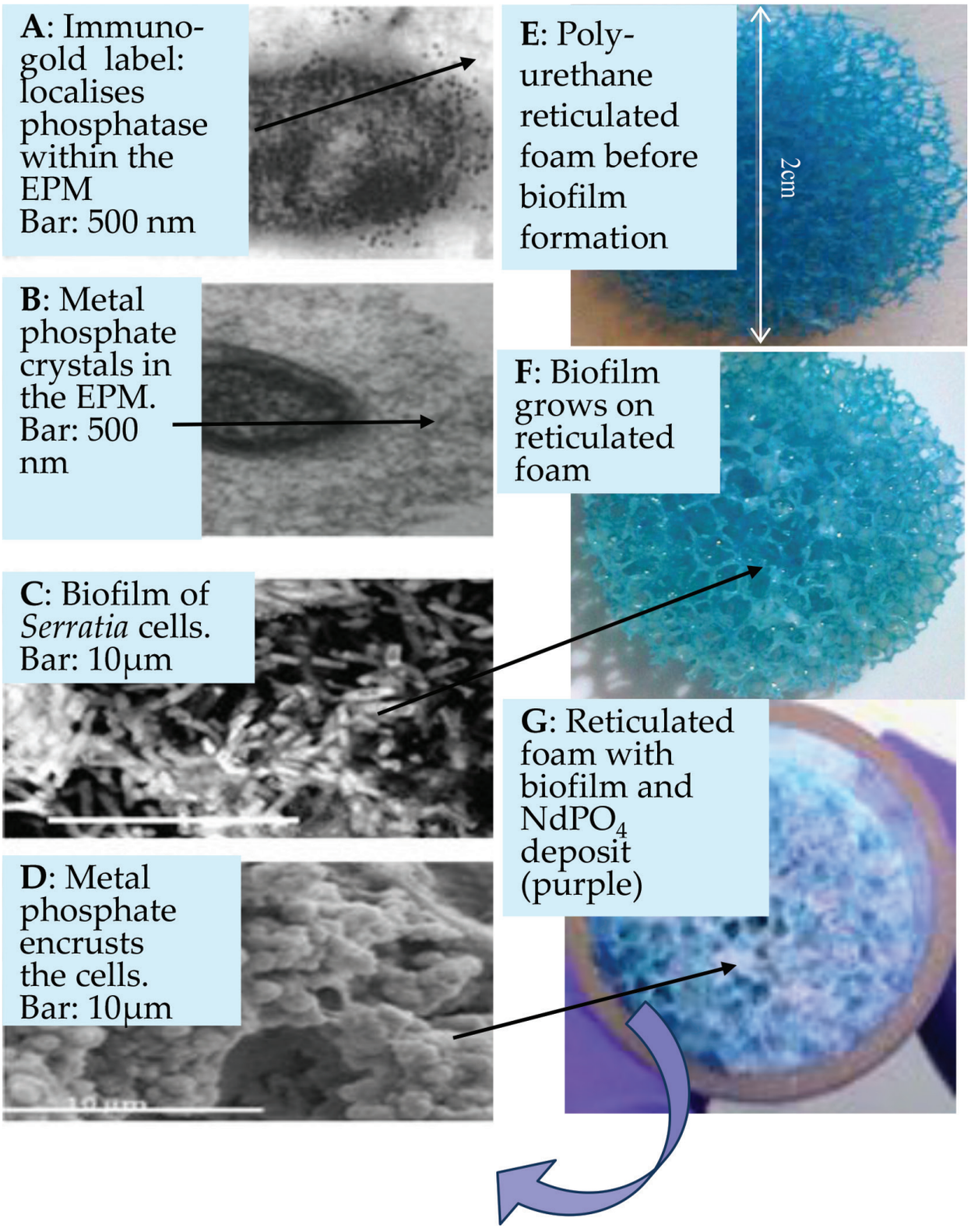


Figure 1. Phosphatase location within the extracellular polymeric material (A) and metal phosphate deposition in EPM (B) by *Serratia* sp. cells. (C and F): Biofilm on reticulated foam discs. (E): foam disc before biofilm colonisation. (D and G): Deposition of $NdPO_4$ after flowing a solution of 1 mM Nd^{3+} and 5 mM glycerol 2- phosphate through a column (seen end-on in G). Blue arrow: Disc as shown in Figure 2.

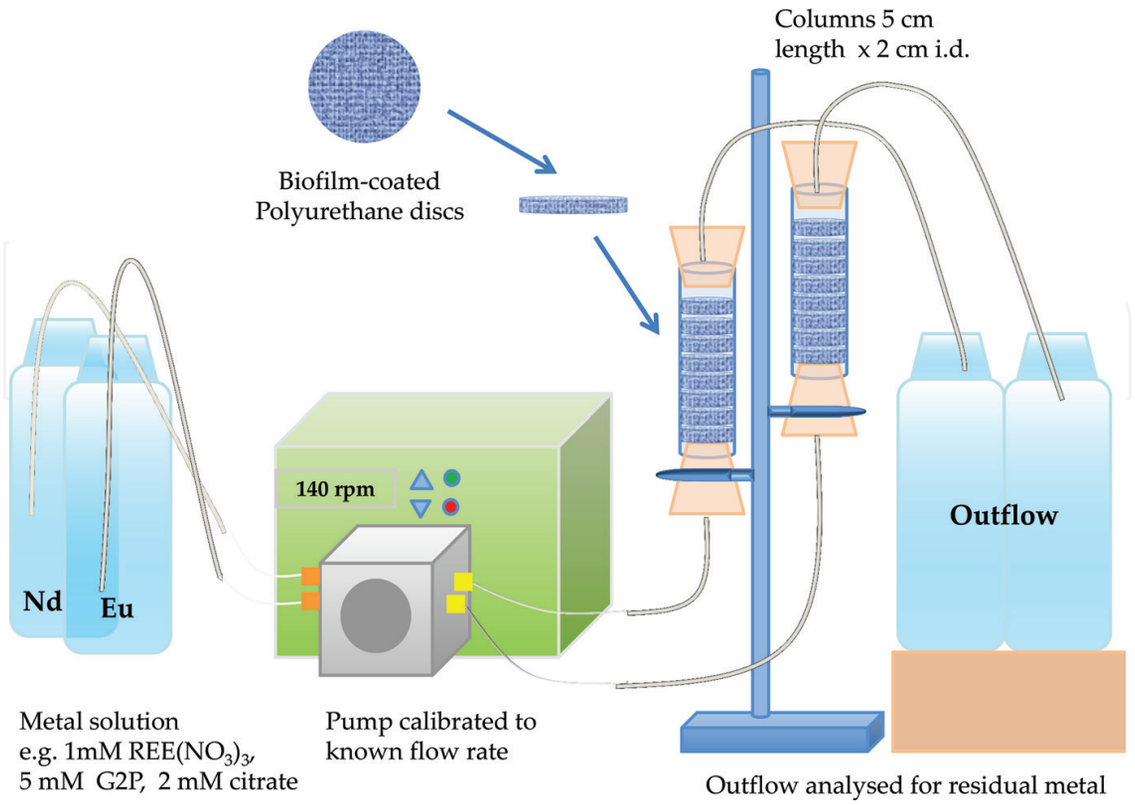


Figure 2. Experiment setup for REE recovery. Column activity is expressed as the flow rate-activity relationship, i.e. that flow rate giving 50% removal of metal under the set conditions. Flow rate-activity ($FA_{1/2}$) value for Nd^{3+} and Eu^{3+} removal by columns was 273 mL/h [21] (see text).

matrix. For example, in the case of U(VI) (and especially Th(IV)) metal hydrolysis occurs extensively with non-chelated metal. This (i.e. loss of OH^- from the solution) promotes a fall in the solution pH as well as formation of metal hydroxide colloids; to forestall hydrolysis and ensure that the experiments were comparable the citrate (as citrate buffer) maintained the required pH.

A working column can be defined in terms of its flow rate activity relationship. A very useful parameter is the $FA_{1/2}$ value which is defined as the flow rate that maintains 50% of the metal removed from the solution. The activity of a column is accurately described as a plug flow reactor and it can be quantified via an integrated form of the Michaelis-Menten equation. This describes the immobilised enzyme component with, in addition, an 'inefficiency' factor which is a lumped parameter describing the additional combined effects of the dissociation of the metal from its citrate complex and metal removal from solution into the precipitate; the latter can be viewed as the propensity of the metal to form a phosphate deposit [30]. However, the actual times taken to attain the multiple equilibria need not be known; they are dynamic in the flow-through system. Some relevant data are reported in non-flow-through systems [31]. The result observed for column activity is the net outcome as a measure of metal removed under a particular condition. In some cases competing reactions may occur. For example, the phosphatase showed transphosphorylation activity (i.e. to regenerate substrate) as shown by using ^{31}P nuclear magnetic resonance (NMR) spectroscopy [32]. It was

found by trial and error that columns optimally require a substrate to metal ratio of more than 2:1. The predictive model was proved in an example of uranium removal, firstly from test solution [30] and then from acidic wastewater from a uranium mine which also contained excess sulphate ion [33]. Importantly, the degree of interference by other components of the flow, such as excess sulphate (or nitrate), can be overcome simply by slowing the flow rate by an amount which can be predicted in a given system [34, 35] to maintain the metal removal at a high level. The effect of the solution pH can be established in a similar way [36]. From this modelling the size of the column required for a particular application can be projected assuming that the major solution components and the pH are known. It should also be borne in mind that, while the activity of different cell preparations differs by within only a few percent, the phosphatase enzyme loses activity while in storage (half-life is 3 months [21]) which needs to be factored-in at the design stage. In practice, a column series would be optimal with fresh columns inserted as required. The phosphatase enzyme is resistant to common inhibitors [37] but has a marked sensitivity to fluoride which is a common component of REE minerals (e.g. bastnäsite, synchysite) and the recently discovered mineral parisite [38].

Polyacrylamide gel-immobilised free cells (pre-grown in carbon-sufficient batch culture) and biofilm (from carbon-restricted culture) were compared with respect to the removal of REE^{3+} from solution. The phosphatase activity is 10-fold less for free cells grown batch-wise than for biofilm cells (250 and 2500 nmol product/min/mg protein). The $FA_{1/2}$ value for REE^{3+} removal was 3.9 and 45.6 mL/h/mg cells, respectively, i.e. an underperformance of ~15% by the gel-immobilised cells which suggests some diffusional constraint within the gel.

3. The need for selective REE recovery against Th(IV) and U(VI) and potential development of the bio-recovery method to metal mixtures

A barrier to exploitation of historic uranium mine tailings (and indeed bottlenecks in primary refining of REE from many minerals) is their widespread occurrence with U and/or Th. For example, at the Elliott Lake site in Ontario, Canada, emphasis has diversified from primary U production to embrace also the untapped REE resource. In 2014, Pele Mountain Resources expanded its business model to include the sustainable development of a low-cost, early-to-market, rare earth processing centre at Elliot Lake (designated as the Eco Ridge Mine Rare Earth and Uranium Project: 'Eco Ridge'); however, this is capital-cost intensive while the price of rare earths has fallen. Hence, an initial monazite processing strategy was adopted (since 2015) for project development at Eco Ridge as the proposed site for Canada's first centre for processing both rare earths and uranium as a low cost alternative to mine development, pending development of sustainable rare earth production and supply chains [39]. Recent market conditions (e.g. a decline in rare earth prices) do not support the development of new hard-rock mining projects *per se* but REE separation is required for the future recovery of REE materials from wastes; hence, establishing rare earth production and separation in countries with primary resources of REE is a first step to supply chain setup.

The Eco Ridge site will start rare earth production by processing imported monazite (REE phosphates), where the high rare earth grades would justify REE production from relatively low ore tonnages. Such an initial 'processing-only' setup would reduce capital outlay and time-to-market as compared to the development of new mine processing operations since the monazite processing facility would then underpin scalable REE production from local resources. Metallurgical techniques for processing monazite are well established (although monazites are fairly resistant to dissolution), and an economic model envisages moving on from monazite to mine tailings.

The foregoing illustrates that 'cleaner' methods to separate REE and U (e.g. in mine wastes) and REE and Th (e.g. from monazite) are needed since current processing methods require multiple hydrometallurgical steps with high consumption of acids and alkalis. It should also be noted that while 'geological' monazite is highly crystalline and hence requires strong acid for dissolution, biogenically recovered monazite comprises nano-crystals of ~14 nm [21] offering a large surface area as compared to native mineral crystals. To re-manufacture monazite biogenically from solution may appear counter-intuitive but the biogenic material would require less onward processing than the primary resource and biological intervention could also offer the potential to separate REE from U and Th.

Initial tests [40] used polyacrylamide gel-immobilised cells, taking into account that both U and Th form tight complexes with citrate (which is needed to prevent the formation of colloidal metal hydroxide deposits). Natural ligands in real systems that fulfil this function would include various organic ligands arising from microbial activities in addition to geopolymers like humic and fulvic acids. Mixed Th(IV)/La(III) and U(VI)/La(III) solutions were passed through columns (25 mL volume) by the method of Tolley et al. [20] at rapid flow rates. Assuming that the time required for the metal-citrate dissociation equilibrium to re-establish following metal removal from the flow into the mineral phase is longer than the flow residence time, it was predicted (according to the relative solubility products, for example this being ~7 orders of magnitude less for the uranium mineral autonite as compared to monazite [9]) that La(III) would be removed effectively while Th(IV) and U(VI) may not. For example, at a flow rate of 198 mL/h (LnF = 5.28 mL/h), the cleavage of the glycerol 2-phosphate substrate was 33%, to give an available phosphate concentration of 1.7 mM. In the metal mixtures, the total metal was 1 mM (0.5 mM of each metal; the metals are described in molar terms to account for the differences in their mass and provide equal concentrations). **Figure 3A** shows that while 100% of La^{3+} was removed from the mixture, the removal of Th was ~20%. In contrast, in another series of tests a higher flow rate was required to 'prevent' U removal (**Figure 3B**), with only a narrow 'window' of flow rates under which 100% of La^{3+} was removed but little uranyl ion.

This narrow flow rate 'window' must be established each time since each waste would contain different components in different proportions and wastes also vary with respect to pH. Hence, while rejection of Th(IV) by the column, and hence metal separation, is feasible using column retention time alone (**Figure 3A**), a better selectivity of REE(III) against U(VI) is required in

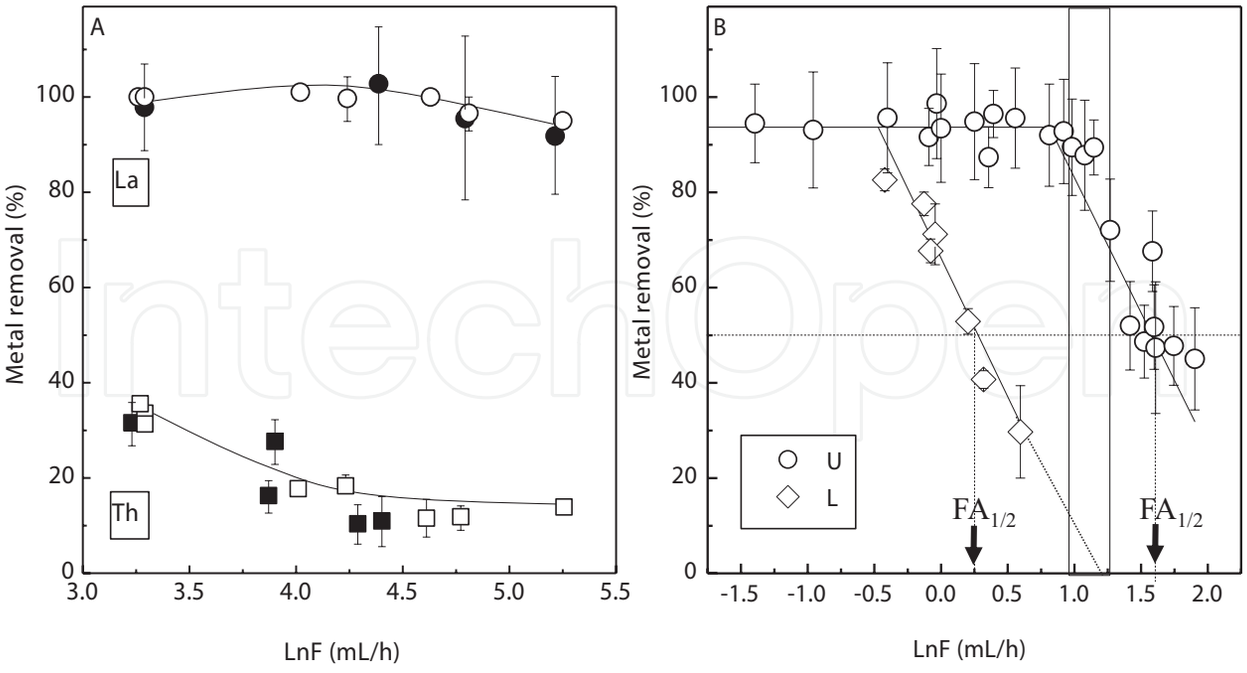


Figure 3. Flow rate-activity relationships for removal of (A) a mixture (0.5 mM of each) of La(III)/Th(IV) and (B) 1mM, separately, La(III)/U(VI) using polyacrylamide gel-immobilised cells in two series of experiments [35]. Closed and filled symbols represent metal only (1 mM) or metal in the mixture (0.5 mM of each). Good separation of La (●, ○) and Th (■, □) is shown in (A). (B) shows a narrow flow rate 'window' at which La^{3+} removal (○) was maintained while UO_2^{2+} removal (◇) was less than 10% (boxed). The concentration of glycerol 2-phosphate was 5 mM (5:1 excess over metal). $FA_{1/2}$ is flow rate giving 50% removal of metal from the flow (arrowed).

order to expand the 'window' of flow rates (**Figure 3B**) between which the former but not the latter is removed. In this respect, an additional complexing agent for UO_2^{2+} could retard its capture within the flow residence time in the column, thereby shifting the flow rate-activity relationship for U(VI) to the left, while leaving the REE^{3+} removal profile unchanged.

4. Biotechnology progress towards selective recovery of REE: the use of biofilm-immobilised cells

The early work used bacteria immobilised in polyacrylamide gel (PAG) [20, 40]. However, gel-systems have insufficient mechanical strength for large scale processes. The *Serratia* cells readily form a biofilm on solid matrices (above) which was used in the removal of $^{235/238}UO_2^{2+}$ from a real nuclear waste [41] as well as Nd^{3+} (**Figure 1G**). Hence, the possible application to selective metal recovery was examined.

Initial comparisons were made using 1 and 5 mM glycerol 2-phosphate (G2P). **Figure 4** shows that, in contrast to gel-immobilised cells, a biofilm-column gave less metal separation e.g. at a removal of UO_2^{2+} of 9.4% (at LnF = 4.96 mL/h) the corresponding removal of Nd^{3+} was 54.2% (at LnF = 4.95 mL/h). This could be attributed to the removal of a selective permeability barrier

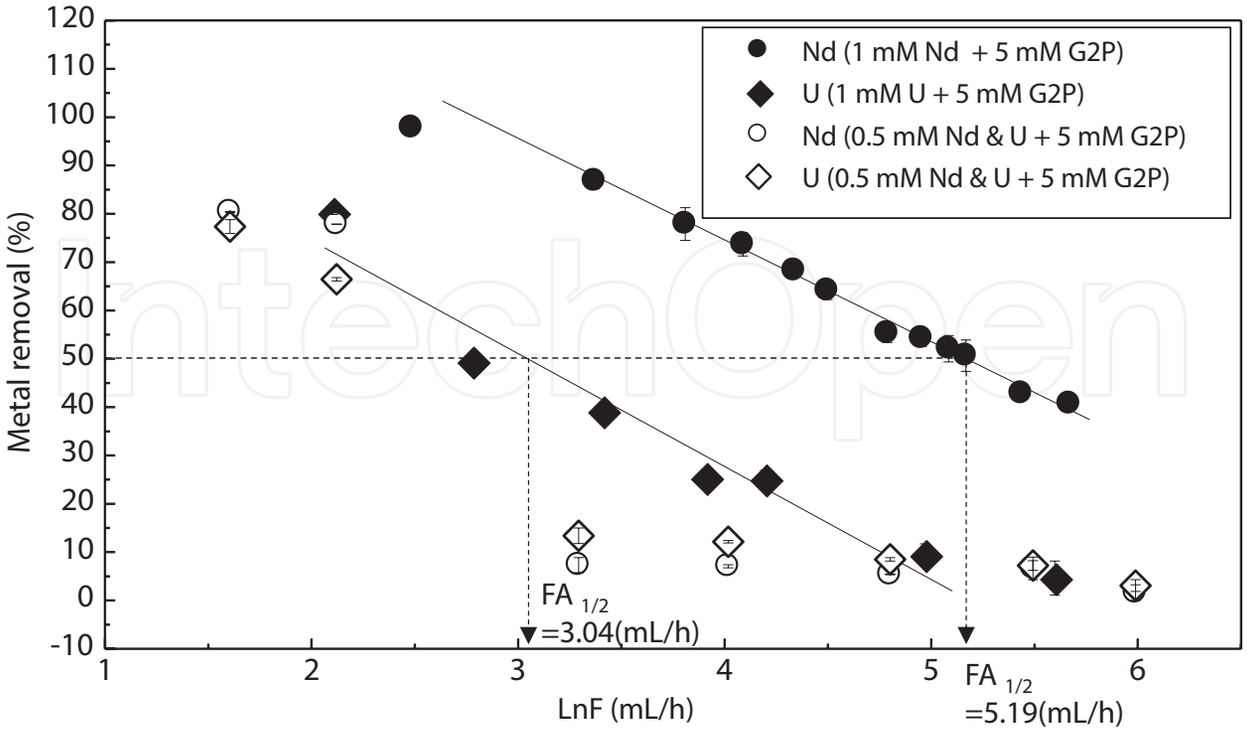


Figure 4. Removal of 1 mM Nd^{3+} (●) and 1 mM (♦) UO_2^{2+} individually from the flow (2 mM citrate buffer pH 5.5; average of two independent biofilm preparations) in separate columns with 5 mM glycerol 2-phosphate (filled symbols and from a mixture containing 0.5 mM of each metal (open symbols). The boxed area is the region of flow rate that confers some selectivity (c.f. Figure 3) as indicated by single metal tests.

in the gel that retarded UO_2^{2+} more than REE^{3+}, to a better permeability of uranyl ion through the natural permeability barrier of the extracellular polymeric materials that characterise a biofilm, or to a combination of both factors.

Removal of Nd^{3+} and UO_2^{2+} in competition with each other is also shown in **Figure 4**. The presence of excess liberated inorganic phosphate was comparable in all cases (not shown) but the mixed metal test shows no selectivity. This was confirmed using 1 mM G2P, i.e. making less free phosphate available (in order to 'starve' UO_2^{2+} of the phosphate it needs to precipitate effectively) did not selectively retard UO_2^{2+} removal.

Comparing **Figure 4** with **Figure 3B**, this study with single metals indicates that biofilm-cells are less effective than gel-immobilised cells in terms of the potential for metal separation. At the $FA_{1/2}$ value for Nd^{3+} (LnF = 5.15 mL/h) the removal of UO_2^{2+} was >20% (**Figure 4**) whereas using gel-immobilised cells the corresponding removal of La^{3+} was ~100% (**Figure 3B**). However, inspection of unpublished data of Tolley [40] (c.f. **Figure 4**) revealed that the removal of La^{3+} by PAG-immobilised cells was depressed to the same level as UO_2^{2+} in the mixture although La^{3+} removal from a single metal solution was >90% at the same flow rate. Hence, clearly the depression of REE removal in the presence of UO_2^{2+} (**Figure 4**) is not attributable to the choice of cell immobilisation method (and hence not attributable to the extracellular polymer produced by biofilm cells). These results show similarities with earlier data of Ohnuki et al. [42].

Here, while Ce(III) was removed onto cells of *Pseudomonas fluorescens* in the presence of citrate comparably to Pr(III) at acidic pH, at pH 6 and above Ce(III) removal was reduced by ~40-fold as compared to La(III) concomitantly with an oxidation of Ce(III) to Ce(IV) observed by XANES spectroscopy. A similar study [42] examining the uptake of Eu(III), Th(IV) and Pu(IV) in the presence of desferrioxamine B (DFO) as a complexing ligand showed that, at pH 6, the removal of Eu(III) was ~6-fold greater than for Th(IV) while the removal of Pu(IV) was ~100-fold less than for Th(IV). Analysis of the oxidation state of Pu was not attempted but it seems possible that partial oxidation of Pu(IV) to Pu(VI) may has occurred in an analogous way to that of Ce(III). In both the Ce(III)/(IV) and Pu(IV)/(VI) tests removal of the mixed valence species was drastically reduced as compared to a single valence species alone. However, this study [42] did not use a mixed metal challenge system, nor was any attempt made to establish the proportions of each metal species in the putative mixture for a single element, nor of the 'preference' of the cells for a particular metal species of that element.

An additional factor in the current study is that the removal of both metals from their mixture failed at rapid flow rates (**Figure 4**) although excess available Pi was confirmed (>4 mM). It is suggested that a large polymeric complex may be formed between the 2 mM citrate and 0.5 mM Nd^{3+}/0.5 mM UO_2^{2+} such that their availability into solution becomes curtailed and metal release into solution may not occur within the column residence time at rapid flow rates. Indeed, in the Pu/DFO/*Ps. fluorescens* system Pu removal was decreased by a further order of magnitude by increasing the Pu/DFO ratio from 1:1 to 1:100 [42], so that less available Pu would be available for interaction with the cells.

Multi-metal polymeric citrate complexes are now well known (e.g. [43]) and can be included in the class of metal-organic frameworks (MOFs) that are gaining increased recognition. Importantly, the structure of the MOF depends on the metals within the complex; a multi-metal citrate framework was shown to assume a cubic crystal structure [44]; many MOF materials have been described [45]. In conclusion, although immobilised bacteria removed metals individually, when metals are combined in the presence of complexing ligands the REE is 'withdrawn' from availability, being captured into a putative bimetallic MOF. Hence, another agent is required that has the potential to compete with putative MOF formation selectively for one metal over another.

5. Biotechnology progress towards selective recovery of REE: use of tributyl phosphate (TBP) as a possible selection tool

The well-established 'PUREX' process uses tributyl phosphate (TBP) to sequester actinides against a background of metal cations. An early study indicated that the complexation of TBP to uranyl ion was more than to REE [46]. Hence, TBP was considered as a possible agent to retard removal of UO_2^{2+} in the REE-accumulating column to enable later recovery of U(VI) downstream. In addition, while effective removal of UO_2^{2}+ from acidic minewater at the expense of glycerol 2-phosphate was achieved successfully [33] a barrier to industrial implementation remains the cost of G2P at scale [47]. This would impact adversely upon commercial REE recovery. As a potential alternative phosphate donor, TBP is cheap and readily

available. These dual advantages prompted evaluation of TBP as an alternative phosphate donor, this requiring, probably, the concerted action of phospho tri-, di- and mono-esterases. On the other hand, since the dibutyl phosphate complex of uranium is insoluble [48, 49] only one enzymatic step might be required, giving DBP (**Figure 5**).

Uranium removal (90%) from acidic U-minewater supported by TBP was achieved by a mixed culture [50]. The column input and output concentrations of TBP were 1.2 and 0.8 mM, respectively; correspondingly, 0.4 mM UO_2^{2+} was removed but the flow rate was very slow (<1 mL/h). The accumulated solid was confirmed to contain HUO_2PO_4 [50] but the presence of other solid uranium species was not sought. As a potential tool for metal separation it is important that TBP does not impact negatively upon REE removal. As confirmed by **Figure 6**, removal of Nd^{3+} was indistinguishable between columns with and without TBP, while the stability of TBP against PhoN phosphatase was shown by an identical release of phosphate under both conditions (**Figure 6**).

Controls established no phosphate leaching from the tubing or materials. With each new flow rate the column was pre-equilibrated before sampling. To check that columns did not require further time to incorporate TBP, up to 20 column volumes were tested at each flow rate. Between experiments, columns were returned to the initial condition (no TBP) to establish stability for re-use in subsequent tests. Data were normalised to factor-in the decay time of the biofilm phosphatase between tests [21]. Total Pi release (open symbols) was calculated as equivalent to Nd^{3+} removal (the solid was $NdPO_4$ [21]) plus that found by assay of soluble Pi. The solid and soluble phosphate data were pooled to give total phosphate liberated. This experimental design was adopted in subsequent tests.

Since TBP was shown to support U-removal by a mixed culture (at a flow rate of 1 mL/h as compared to >200 mL/h by using G2P, above), it may be expected that a tight binding of uranyl ion to TBP would slow the rate of the precipitation reaction with phosphate liberated

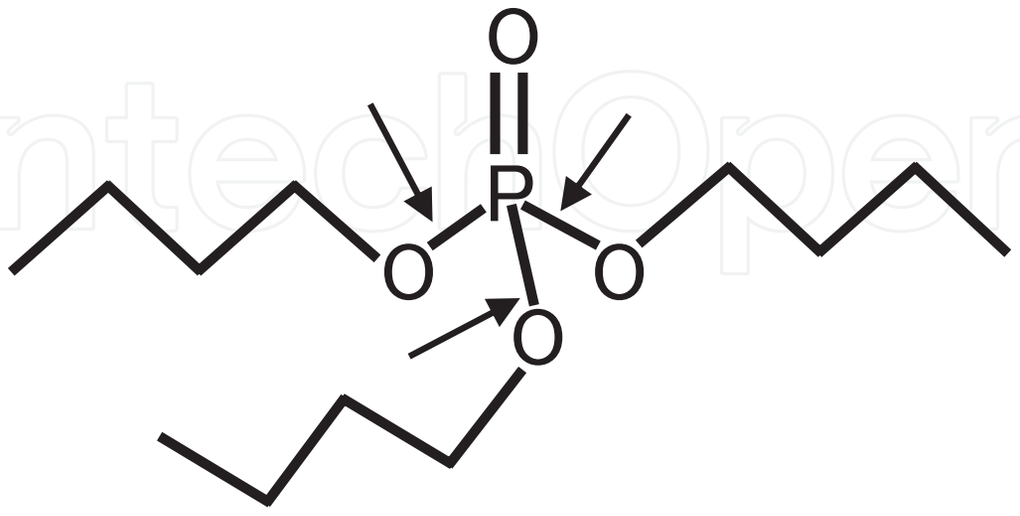


Figure 5. The structure of tributyl phosphate (TBP). Note that, unlike with glycerol 2-phosphate (G2P), three phosphoester bonds (arrowed) require cleavage to yield free inorganic phosphate (Pi) via intermediate DBP. The products would be 1 mol of Pi and 3 mol of butanol. The enzymology is unknown.

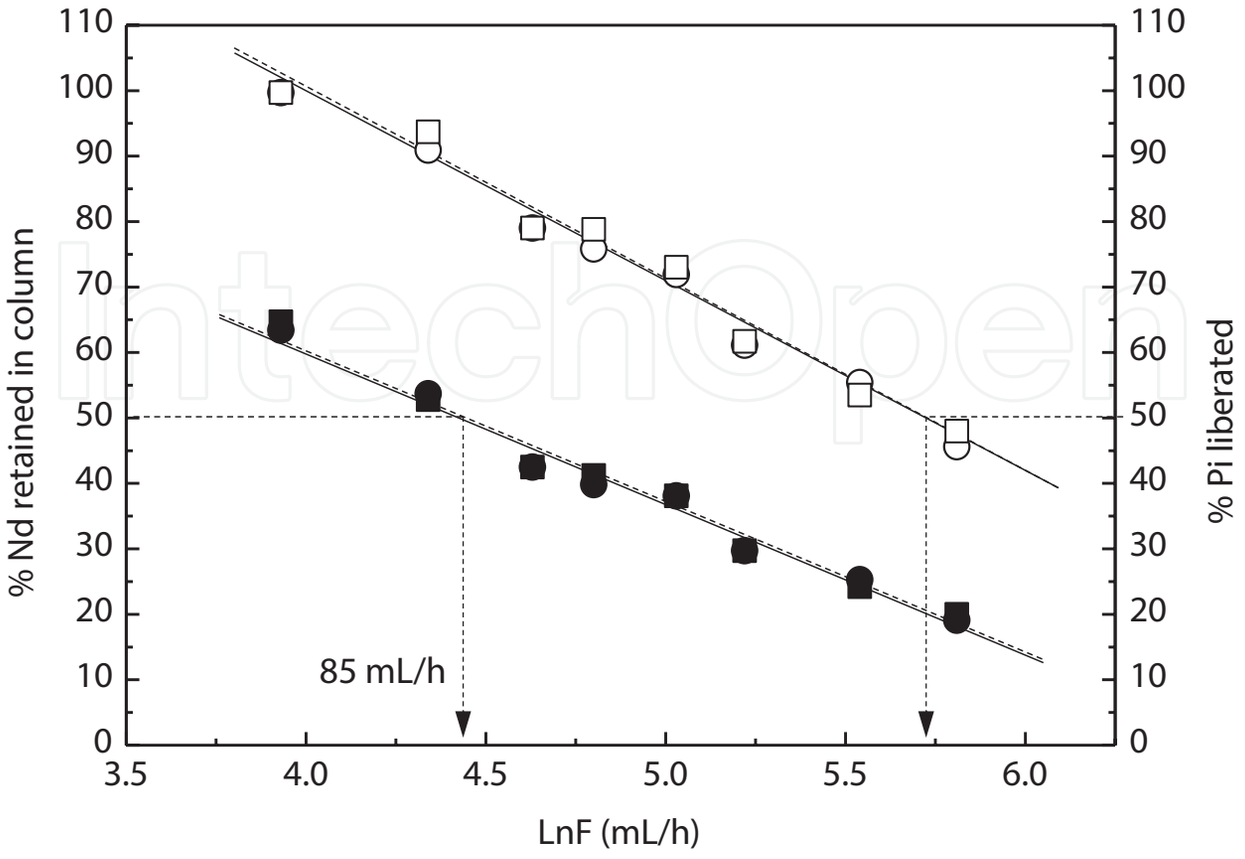


Figure 6. Effect of TBP on Nd^{3+} removal. Biofilm-foam discs (8) were packed into glass columns (Figure 2). Each column received an equivalent mix of discs from positions in the growth vessel. Tests used biofilms made from two preparations (variation <5%). Solution (1 mM G2P, 1 mM Nd^{3+}, 2 mM citrate, pH 5.5 (●, ○)) was passed upwards at varying flow rates. TBP (2 mM Alfa Aesar, fresh), was supplemented directly into the solution and agitated vigorously to maintain an aqueous suspension (■, □). Open symbols: Pi liberated. Filled symbols: metal removed.

from G2P in the bulk solution (by maintaining a low concentration of free UO_2^{2+}), but, bound to TBP, the uranyl would be held adjacent to any liberated DBP for removal in a slower flow rate column downstream.

An early study indicated the ability of cells of *Serratia* sp. strain N14 to hydrolyse TBP [51]. However, the phosphatase also behaved as a transphosphorylase regenerating alkyl phosphate substrate from the alcohol product in a futile cycle [32] in the absence of a 'phosphate trap' such as a heavy metal ion. However, the breakdown of TBP was genetically unstable [52]. Later work [53] showed that degradation of TBP by *Serratia odorifera* occurred via co-metabolism of a primary substrate that involved neither the release of detectable di-butyl or mono-butyl phosphates nor of Pi. These authors subsequently identified an oxidoreductase activity in *Rhodobacter palustris* that was implicated in TBP breakdown, also noting that oxidoreductases do not necessarily require molecular O_2 but can utilise the oxygen present in water [54]. In this context two salient features prompted this current study: (i) the breakdown of TBP in highly radioactive solution (radiolysis) proceeds via chemical formation of dibutyl phosphate from TBP [48] (presumably via free radical attack from radiolysis of water); the DBP forms insoluble metal precipitate (see above) and (ii) the *Serratia* phosphatase shows

bi-functional phosphohydrolase and oxidoreductase activities and was found to generate free radicals [55], this bi-functionality resembling a reported vanadium peroxidase [56].

Application of the bacteria to support metal removal via trialkyl phosphate breakdown was studied empirically in early work using Cd^{2+} as the phosphate trap [57]. The column (*Serratia* cells immobilised in polyacrylamide gel; this strain N14 was originally designated as a *Citrobacter* sp. in early work) was challenged with 2 mM Cd^{2+} with limiting concentrations of glycerol 2-phosphate: 1 or 0.5 mM; the former supported 50% removal of 2 mM Cd^{2+} (i.e. leaving 1 mM available Cd^{2+}) while 0.5 mM G2P supported ~30% of 2 mM Cd^{2+} (**Figure 7**). With 0.5 mM G2P/5 mM G2P alkyl phosphate (1:10), the removal of Cd^{2+} fell rapidly to the 'baseline' level of 0.5 mM G2P alone. A mixture of 1:4 gave a slower loss of activity in each case (**Figure 7**) with a flow of 2–3 L sustained before the 'baseline' attributed to 0.5 mM G2P alone was reached. However, a mixture of 1 mM G2P:2 mM TBP supported steady state removal of 70, 75 and 90% of the Cd^{2+} (i.e. this accounted for more phosphate consumed than was accountable as the Pi liberated from G2P) using trimethyl, triethyl and tributyl phosphates, respectively (**Figure 7**). For 90% of 2 mM Cd^{2+} to be removed (i.e. 1.8 mM) with, maximally, 1 mM Pi able to come from the G2P (i.e. 1 mM G2P provided in the inflow) the implication is that 0.8 mM Pi had been liberated from TBP (from 2 mM TBP provided).

This early study [57] offered no explanation for the observed behaviour but the requirement for G2P to facilitate TBP breakdown is in accordance with a hypothesis of co-metabolism proposed

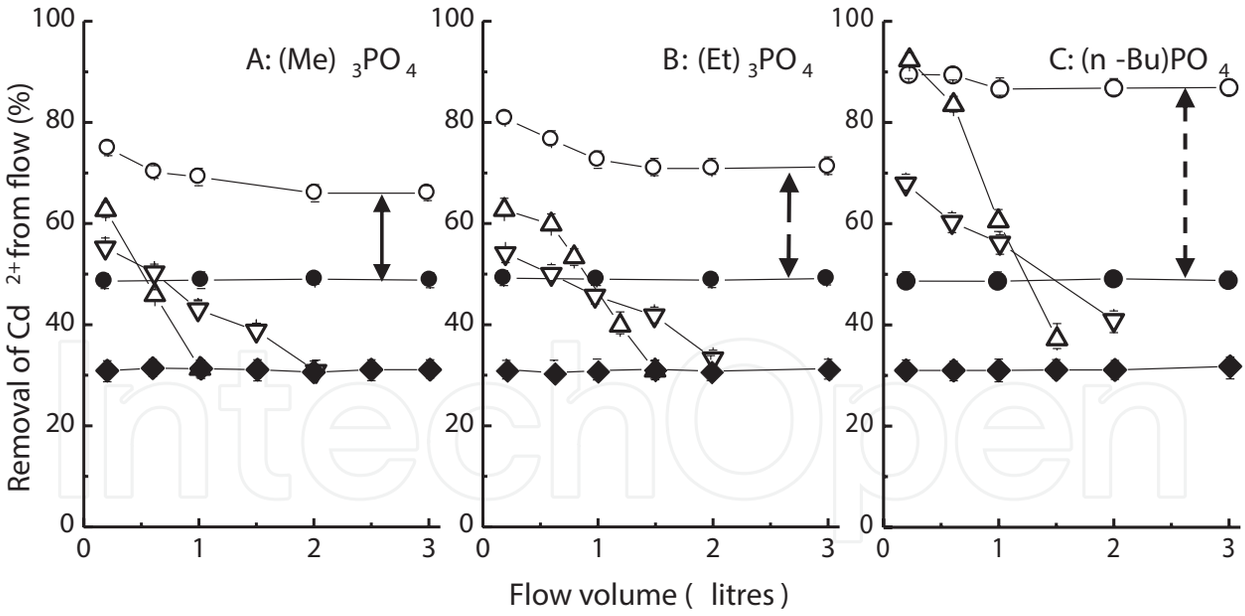


Figure 7. Ability of trialkyl phosphates to support removal of Cd^{2+} from solution by polyacrylamide gel-immobilised cells with and without added glycerol 2-phosphate (G2P). Data are redrawn from Ref. [57]. The flow rate was 30 mL/h (column working volume 60 mL) with 2 mM Cd^{2+} and 1mM (●), (50% removal of Cd^{2+}) and 0.5 mM (◆) (30% removal of 2 mM Cd^{2+}) G2P. Mixtures were also supplemented with 0.5 mM G2P/5 mM alkyl phosphate (ratio of 1:10; total phosphate was 5.5 mM) (△) or 0.5 mM G2P/2mM alkyl phosphate (ratio of 1:4; total phosphate was 2.5 mM (▽) or 1 mM G2P/2 mM alkyl phosphate (ratio 1:2; total phosphate was 3 mM) (○). Trimethyl phosphate supported removal of additional ~30% of Cd^{2+} (A: solid arrow); triethyl phosphate, of additional ~40% of Cd^{2+} (B: broken arrow) and tributyl phosphate, of additional ~80% of Cd^{2+} (C: dashed arrow) at steady-state.

by Berne et al. [53, 54]. This requires that the co-product of G2P hydrolysis, i.e. glycerol, is metabolised by the cells and this was confirmed by analysis of the exit solution of metal-accumulating columns where not only glycerol but also citrate was consumed by the cells (P. Yong, M. Paterson-Beedle and L.E. Macaskie, unpublished). Under metal-accumulating conditions, the non-growing cells accumulated large deposits of polyhydroxybutyrate as a carbon and energy stored (see later) [58]. The early work [57] showed several salient features; G2P was required for utilisation of TBP (**Figure 7**) and 1 mM TBP supported a stable column. On the other hand, 0.5 mM G2P was insufficient to sustain metal recovery (**Figure 7**). Moreover, columns were 'refreshed' by a period of TBP-free flow followed by a new TBP-supplemented cycle [57], in accordance with not only a role for co-metabolism (of glycerol) as proposed by Berne et al. [53] but to replenish PHB reserve during 'refreshment' to support the next TBP cycle. Also, addition of the proposed alcohol end-product (3-fold molar excess to alkyl phosphate) inhibited metal removal [57] in accordance with a competing transphosphorylation (above) of phosphate onto liberated alcohol [32]. The removal of Cd^{2+} supported by trimethyl and triethyl phosphate was reduced by ~25–30% by addition of methanol and ethanol, respectively, and by 20% in the case of TBP/butanol [57].

A hypothesis was formulated to widen the flow rate 'window' boxed in **Figure 3**. This assumes that REE^{3+} forms a weaker complex with TBP than does UO_2^{2+} [46]; no benefit for REE removal would be anticipated with TBP (**Figure 6**) if REE^{3+} is presumed to be not in close association with TBP or its breakdown products. Rare earth phosphate ($REEPO_4$) formation is rapid and hence occurs at high flow rates while UO_2^{2+} requires more time to form a precipitate [21]. As UO_2^{2+} complexes with TBP, it is ideally placed to capture liberated phosphate (or DBP) from TBP breakdown to form uranyl phosphate precipitate in advance of the competing transphosphorylation reactions of phosphate onto liberated alcohol. Hence, incorporation of TBP into a REE/U(VI) G2P/TBP mixture might better capture $REEPO_4$ at a rapid flow rate while rejecting uranyl, which would be available for downstream recovery as uranyl-DBP at a slower flow rate.

However, as shown in **Figure 8**, with 1 mM G2P/2 mM TBP (combination as used in the early work [57]; **Figure 7C**) there was no selectivity of metal removal and, indeed, the removal of both metals was inhibited even at slow flow rates. With 5 mM G2P/0.5 mM TBP both metals were removed at slow flow rates (below 10 mL/h) but with little or no selectivity between them. In the absence of uranyl ion, Nd^{3+} appeared to be resistant to this inhibition at all flow rates (**Figure 3**) and it may be suggested that, once they are in a presumptive bimetallic citrate-MOF, the effect of TBP applies to both metals equally.

Hence, despite promising early work using La^{3+} and UO_2^{2+} separately (above) and a successful TBP supplement being shown to boost metal recovery by gel-immobilised cells (**Figure 7**), TBP was ineffective to support metal removal from a single metal or mixed Nd/U flow using biofilm-cells for reasons still to be established. In this context, it is noteworthy that other work using triethyl phosphate as a means for generating inorganic phosphate gave dissolved phosphate at concentrations far in excess of that based on equilibrium consideration but there was no detectable mineral precipitation [59]. Both metal speciation and full mass balances would form the basis for future work to shed light on these anomalies.

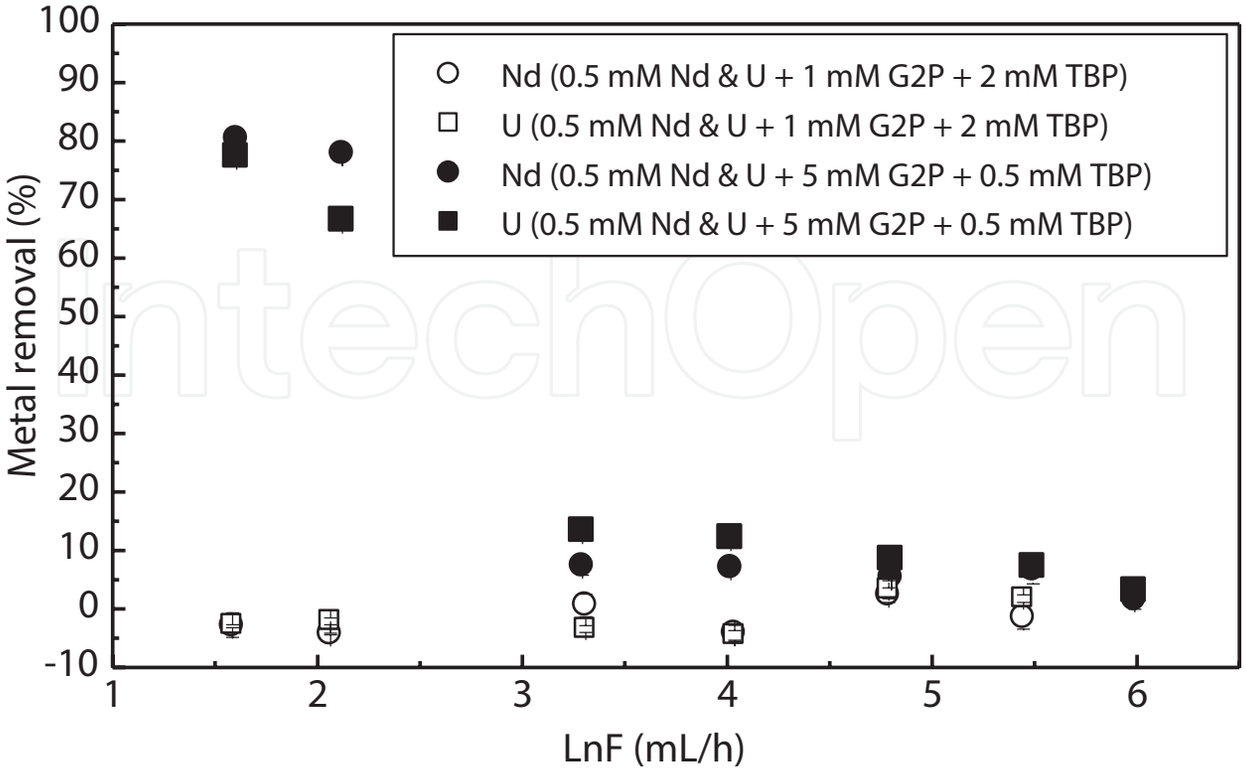


Figure 8. Removal of Nd^{3+} (●, ○) and UO_2^{2+} (■, □) from a mixture of 0.5 mM of each metal in flow with 1mM G2P/2 mM TBP (open symbols) or 5 mM G2P/0.5 mM TBP (filled symbols).

If MOF formation is confirmed, this has implications for the treatment of wastes more generally which contain organic complexing agents, e.g. those arise naturally from degradation of larger polymers [60]. In the case of uranyl removal, the use of bicarbonate ion to remove UO_2^{2+} out of the immobilised phosphate mineral in a column pre-loaded with HUO_2PO_4 was shown [30]; hence, addition of dilute bicarbonate and use of a second uranium-accumulating column could provide an alternative/supplemental route to U-retardation with downstream acidification to convert HCO_3^- to CO_2, releasing UO_2^{2+} as a free ion available for phosphate bio-mineralisation; the enzymatic bio-mineralisation is tolerant to pH down to pH 4 [33, 36] but further developmental work is required.

6. Potential for recovery of REE from bio-mineralised columns

A process for REE bio-refining into new materials would require additional processing steps. REE recovery from the bio-REE phosphate bio-material could use NH_4^+ since this has been shown for REE leaching from clay minerals and metallic scraps [61–63]. The highly nanocrystalline nature of bio-$REEPO_4$ [21] (see later discussion) would make it suitable for a more 'benign' leaching than the strong acids required for 'geological' monazite minerals. A series of tests using columns supplemented with acidic 100 mM $(NH_4)_2SO_4$ (to simulate leach liquor) showed that this had no effect on column activity at pH 5.5 (**Table 1**), with only a slight loss

	pH 5.5	pH 3.5	pH 5.5 (return)
Without/with (±) 100 mM $(NH_4)_2SO_4$	±	±	±
$FA_{1/2}$ (mL/h)	38/38	19/17	30/25

Columns were run at pH 5.5 or 3.5 with and without $(NH_4)_2SO_4$. After determination of $FA_{1/2}$ they were returned to the standard condition (pH 5.5 without $(NH_4)_2SO_4$) to check for column robustness, with 3–6 wash volumes before sampling. Data from Ref. [64].

Table 1. The effect of 100 mM $(NH_4)_2SO_4$ on Nd^{3+} recovery (percentage of 1 mM input metal removed) by 10–11 month old biofilms at pH 5.5 and 3.5.

of activity (~10%) seen after exposure to pH 3.5 and return to pH 5.5. Columns were returned to the original conditions after each use to check that the potential for column re-use was not compromised for potential re-use in multiple cycles.

7. An alternative approach for REE recovery via biogenic phosphate

Uptake of Ce(III) was reported by the Gram negative microorganism *Pseudomonas fluorescens* [65]. Ce(III) uptake was accompanied by its oxidation to Ce(IV). A 10-fold increase in the number of bacteria present reduced the proportion of Ce(IV) formed, from 80 to 50%, suggesting a mechanism of 'fixation' of the Ce(III) into a form on the cells which was resistant to oxidation. A longer contact time resulted in a greater amount of the 'fixed' Ce(III) following addition of MnO_2 as an oxidising agent. Cerium phosphate nano-particles were formed on the cells in the absence of added phosphate and hence the formation of Ce(III) phosphate at the expense of stored and mobilised phosphate was suggested [65]. Accordingly, storage of phosphate as intracellular polyphosphate bodies in *Pseudomonas putida* has been reported [66].

Ohnuki et al. [65] suggested two mechanisms of Ce(III) uptake, a rapid sorption followed by a slower Ce(III) PO_4 deposition. Analysis by time resolved laser fluorescence spectroscopy (TRLFS) that showed that the initial adsorption of Eu(III) on Gram negative *Ps. fluorescens* occurs through multi-dentate and inner-sphere complexes [6], while X-ray extended fine structure (EXAFS) analysis of Sm^{3+} uptake by Gram positive *Bacillus subtilis* showed that Sm^{3+} is complexed with carboxylate and phosphate functional groups [8].

The conclusion regarding a secondary, slower process of REE(III) fixation via phosphate deposition via stored reserves is in accordance with the earlier results. Jiang et al. [9] observed formation of Ce(III) and Yb(III) phosphates by the yeast *Saccharomyces cerevisiae* over 2 days. When lysed for 2 months after development, $YbPO_4$ nano-particles persisted in the solution showing the stability of the nano-material [9]. Jiang et al. [9] attributed this to the very low solubility product of REE phosphates (e.g. $CePO_4$ log $k = -26.2$) as compared to, for example, uranium minerals (e.g. for autonite log $k = -19.3$ [9]).

Up to date, apart from the *Serratia* immobilised cell system (above), there has been little attempt at bio-process development using bio-mineralisation systems. Delivery of the mineralising

microorganisms into the target solution and separation of the harvested REE phosphate does not seem to have been developed apart from the use of immobilised biomass columns. It should be noted, however, that while the *Serratia* enzymatic mechanism was irreparably damaged at pH 3.5 and below [64], Yb phosphate mineralisation by *S. cerevisiae* occurred at pH 3 (although the longevity was not tested). EXAFS analysis of the deposited material showed a similar Yb(III)-edge for samples made at pH 4 and 5 while that for sample made at pH 3 was subtly different [67].

8. An alternative biotechnology for REE recovery: use of biogenic hydroxyapatite

Hydroxyapatite (HA), a major component of natural bone, has been used as a material for sequestering radionuclides using bone-HA [68]. However, use of animal by-products is subject to legislative constraints [69]. Using the same mechanism as described for phosphatase-mediated deposition of $NdPO_4$, (above) deposition of biogenic hydroxyapatite was achieved using biofilm-immobilised cells [70]; use of biofilm, as described above, yielded a highly adhesive bio-HA layer [71] which was tightly held onto the support after HA-mineralisation The work done to remove biofilm from a polypropylene support was measured (using a micromanipulator) at 3.4 ± 0.7 and 126.2 ± 23.3 J/m^2 for native and bio-mineralised biofilm, respectively [71].

The *Serratia* bio-HA was found to accumulate Eu^{3+} [72, 73]. This study focuses on the formation of cell-bound HA-crystals with the aim to produce smaller crystallites than those obtained by 'classical' methods which include batch growth of bacteria as used previously [74, 75]. Previous work on the bio-deposition of $NdPO_4$ by continuously pre-grown cells showed that, despite extensive bio-mineralisation, an average crystallite size of ~14 nm was obtained [21]; the cells apparently exert a stabilising effect that restricts 'runaway' crystallisation and nanoparticle agglomeration. One rationale for this is that, since continuously pre-grown cells produce copious extracellular polymers and since these polymers provide nucleation sites [76], cells pre-grown under continuous culture should produce more and smaller (for the same amount of Ca^{2+} provided) crystals than batch-grown cells, being stabilised against agglomeration by the surrounding extracellular polymeric material (EPM) matrix. A biofilm comprises cells bound together via copious EPM [68], the composition of which is dependent on the growth conditions [76, 77]. It is well known that Ca^{2+} ions crosslink adjacent EPM chains via their carboxyl groups and, in this respect, the bacterial EPM-Ca (subsequently EPM-HA) complex could be considered as a biogenic metal-organic framework (MOF), supplemented with ingressing phosphate via the co-localised phosphatase enzyme resulting in localised nanoprecipitation under bio-control. Since bio-HA on *Serratia* was shown to take up Eu^{3+} (above), this prompted a study of the use of this material as a potential scavenging agent for REEs which does not require the use of living cells. Dried, heat-treated bio-HA accumulated metals as well as fresh (hydrated) bio-HA [73] give a bio-mineral with a long shelf-life and less encumbered by restrictions on use as compared to animal by-product materials.

The material deposited in the biofilm within the EPM (**Figure 9A**) and biofilm between the cells (**Figure 9B** and **D**) was confirmed to be hydroxyapatite using selected area X-ray diffraction and X-ray powder diffraction analysis (XRD) [78] and estimation of the bio-HA nanoparticle size by the XRD patterns under various incubation conditions gave an average of 20–25 nm [78, 79] as compared to the ~40 nm made by batch-grown cells [75] and ~80 nm of commercial hydroxyapatite (**Table 2**) [73].

Two features are highlighted by **Figure 9**. It is known that the bacteria metabolised the carbon components of G2P and citrate as provided in the mixture (analysis showed the disappearance of both citrate and glycerol P. Yong, M. Paterson-Beedle and L.E. Macaskie, unpublished); in the absence of any nitrogen source the cells did not grow but instead deposited intracellular deposits of the storage material polyβ-hydroxybutyrate [58] as shown by the electron

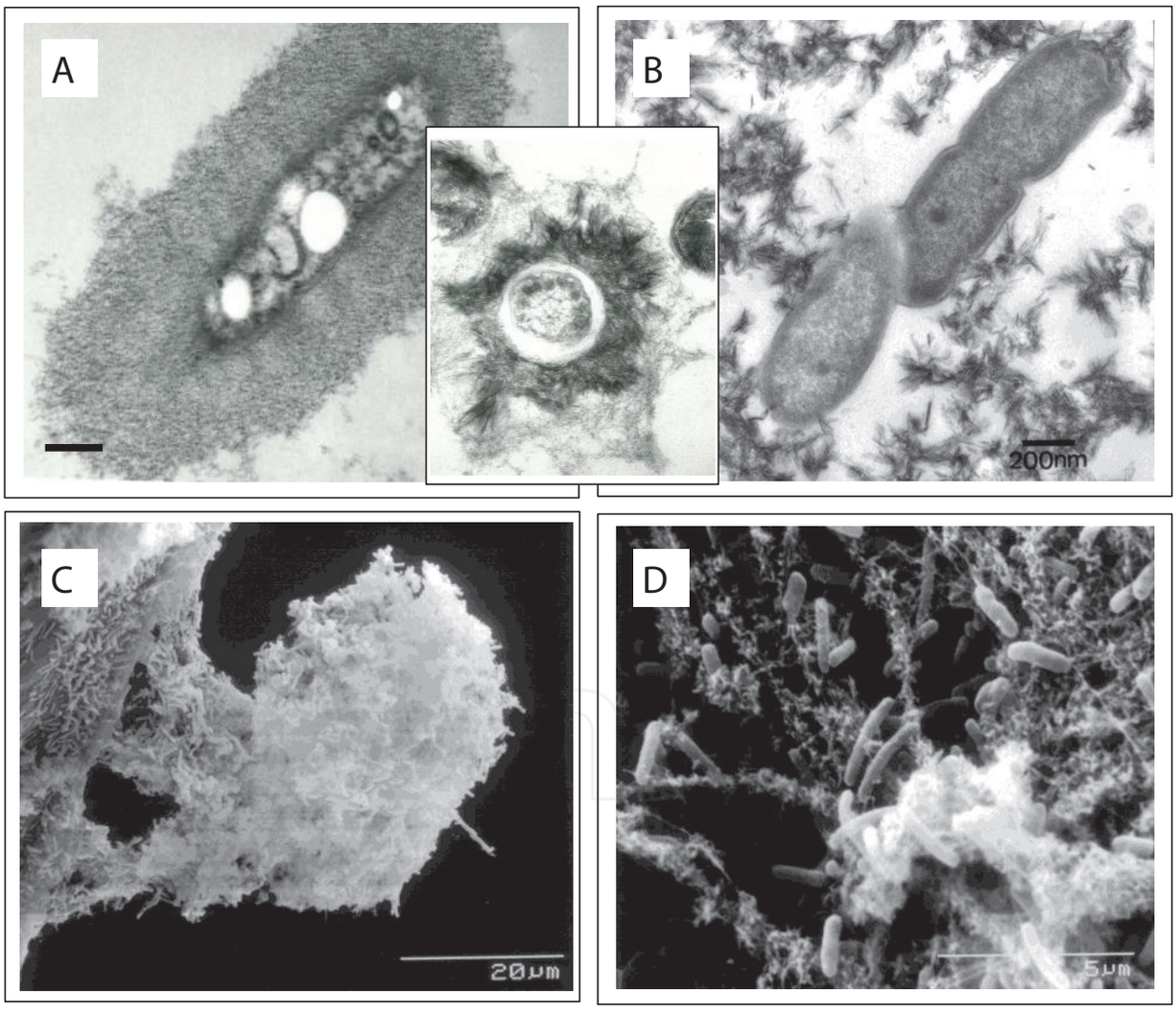


Figure 9. Formation of hydroxyapatite (HA) by *Serratia* cells. (A) Initial deposition of HA nano-crystallites within the EPM layer surrounding the cell. (B) As HA deposition proceeds (via daily dosing of Ca^{2+} and G2P) the material assumes needle-like deposits of HA extruding from the cells. Inset: Progression of the bio-HA (cross section) from cell-bound to needle-like crystals within layers of EPM Images: transmission electron microscopy; bars = 200 nm. (C) Mass of bio-HA from cut spur of polyurethane foam. (D) Top view of HA-biofilm on foam. Note extensive mineralised deposits cross linking the layer of cells (images: scanning electron microscopy).

Treatment (°C)	Organic content (%)	Surface area (m^2/g)	Crystallite size (nm)	Uptake of metal (mmol/100 g material)	
				Eu^{3+}	UO_2^{2+}
20	36	ND	40	154	131
200	27	65	34	154	131
250	23	76	37	154	131
300	16	93	31	154	131
350	9	102	37	154	131
400	7	115	36	154	131
450	3	86	36	154	131
500	3	61	32	154	131
550	1	38	48	154	131
600	2	27	64	154	131
650	0	17	125	153	124
700	0	12	271	151	116
Comm-HA	0	21	85	13	130

Data from Handley-Sidhu et al. [73]. Bio-HA was made by daily dosing with 2 mM Ca^{2+}, 5 mM G2P and 2 mM citrate buffer in 0.1 M AMPSO buffer, pH 8.6. Comm-HA: commercial HA (Sigma-Aldrich). Metals were used at 10 mM individually (aq; pH 5–6); no mixed metal tests were carried out. Eu uptake was 0.23 mg/mg bio-material (0.32 mg/mg HA component); U uptake was 0.31 mg/mg bio-material (0.42 mg/mg HA component) i.e. ~30 and 40% of the mass of the native bio-HA, respectively. Errors were within 5%.

Table 2. Uptake of Eu^{3+} and UO_2^{2+} into bio-HA pre-treated at increasing temperatures.

transparent inclusion bodies in **Figure 9A**; the degree of carbon turnover was not established. Secondly, the pattern of bio-HA deposition was shown as an initial formation of electron opaque material in the EPM around the cell (**Figure 9A**; capsular material, after 3 days of daily dosing with Ca^{2+} and G2P), progressing to intense mineral deposition within the EPM and formation of needle-like crystals that egressed around and beyond the cells and in the looser EPM in the regions between them, and densification to form a mineral network (**Figure 9B** and **D** and inset). Examination by scanning electron microscopy (a cut end of the foam is presented) shows the role of biofilm in adhering bio-HA to the support (**Figure 9C**) and in addition mineralised strands of EPM are visible between the cells and crosslinking them (**Figure 9D**). Many of the cells have become separated from the EPM-HA matrix leaving a meshwork of HA strands (**Figure 9D**)—a MOF that is typified by a crystalline material with voids to permit solute permeation. The biomaterial was evaluated for its ability to take up Eu^{3+}.

9. Eu^{3+} uptake by bio-HA made by cell suspensions

Early work used cells that had been pre-grown in batch culture suspensions (no carbon restriction). This reduces their ability to form biofilm (and hence EPM) [77] and hence continuously pre-grown and carbon-restricted cells were routinely adopted and bio-HA was made by daily

dosing of re-suspended cells with a mixture of Ca^{2+}, G2P and citrate. Initial studies established that bio-HA made in the presence of citrate was more efficient than commercial HA in removing Sr^{2+} from an artificial groundwater [74] and hence citrate (generally 2 mM) was routinely incorporated into the Ca^{2+}/G2P challenge solution to make bio-HA. Following initial work by Holliday et al. [72] a subsequent study provided Eu^{3+} to a preparation comprising 26% organic material and hence 64% loading of HA (20 mg mass of bio-HA) (**Table 2**); the uptake of Eu^{3+} was ~30% of the HA dry mass (**Table 2**). Heating of the HA materials showed that bio-HA was little-affected even after removal of the organic component and potential agglomeration of the nano-crystallites and with a significant reduction in their surface area (**Table 2**). This suggested a mechanism other than simple surface adsorption and it was also noteworthy that while UO_2^{2+} was removed comparably by the bio- and commercial-HA, the latter showed negligible ability to remove Eu^{3+} which suggested differences in the nature of biogenic and chemical HA materials.

In a subsequent study (daily dosing with mixtures of $CaCl_2$, G2P and citrate at pH 7.0, 8.6 or 9.2: 8 days; all of the Ca^{2+} was removed each day) a known mass of bio-HA was made onto a known mass of bacteria (to give 50% loading as HA); here, the Eu^{3+} uptake reached ~42 mg/100 mg bio-HA or 0.84 mg mineral (i.e. 84% of the mineral mass) [78]. The HA-crystallite size was 21 ± 1.6 nm from materials made at pH 7 and 8.6 (pooled data) [79].

Comparing HA-bio-material made at pH 7, the optimal mixture was 2 mM Ca^{2+}, 2 mM citrate and 5 mM G2P [79] (5:2 of G2P:Ca^{2+}) and changing this ratio to 1:5 reduced the capacity for Eu^{3+} substantially (**Figure 10**).

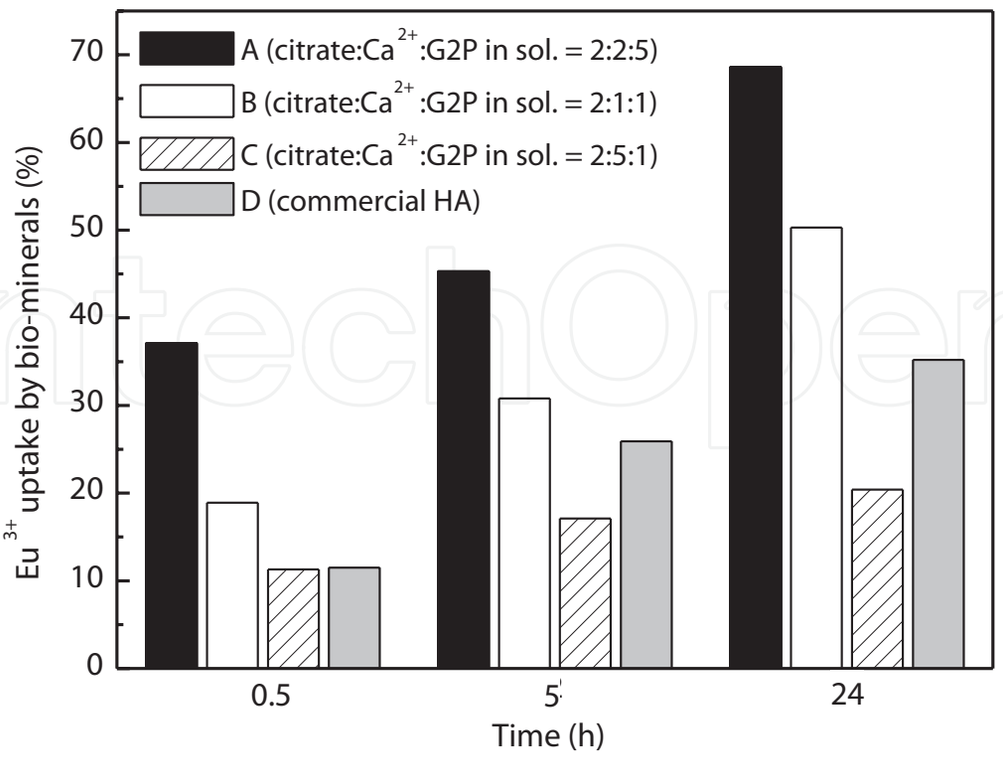


Figure 10. Uptake of Eu^{3+} made by bio-HA at pH 7 by methods A, B and C of bio-HA synthesis prior to Eu^{3+} challenge [79]. No further uptake occurred after 24 h solution (sol.) mixtures (citrate:Ca^{2+}:G2P) A: 2:2:5; B: 2:1:1; C: 2:5:1; D: commercial HA.

10. Eu^{3+} uptake by biofilm-HA immobilised in flow-through columns

The biofilm component of the continuously pre-grown bacterial culture was retained for use in this study (column tests). The planktonic cells fraction (from the vessel outflow) was used in previous work [78, 79]. Cells were from two independent cultures (I and II). Biofilm from the continuous culture vessels as immobilised biofilm-HA in a flow-through column. In order to be able to compare the results with a previous biofilm-HA adhesion study that quantified and confirmed the strength and durability of biofilm-HA [71], the biofilm was loaded with HA at pH 9.2. The HA-loading was calculated (by loss of Ca from the column exit solution) to be ~5 times the dry weight of bacteria (2300 mg of HA per column of eight biofilm discs). Following loading with HA and washing, the columns were challenged with 0.5 mM $Nd(NO_3)_2$ (aq) at 4 mL/h (0.5 column fluid vol/h). The exit solution was monitored and the Eu^{3+} breakthrough point was determined (**Figure 11**).

The bio-HA columns (but not the control) removed Eu^{3+} (~95%) during 2 L after which the activity decreased. The breakthrough region was ~2 L with a large data scatter after ~2.4 L. The column was not saturated since Eu^{3+} removal was sustained at ~50% removal until 4 L (mean value: **Table 3**) when the experiments were stopped. A mass balance analysis was calculated by averaging each point for experiments I and II and then calculating the mean of all samples between 2 and 4 L of flow. Initially (up to 600 mL) some phosphates was evolved which suggests a release of loosely bound HA material. From 600 mL to 2 L this was 0.1 mM which, subtracted from the Ca^{2+} released, indicates stoichiometry between Eu^{3+} removed and Ca^{2+} evolved and hence an ion exchange mechanism. The 1:1 stoichiometry was clearly seen in the second flow period (2–4 L) (**Table 3**).

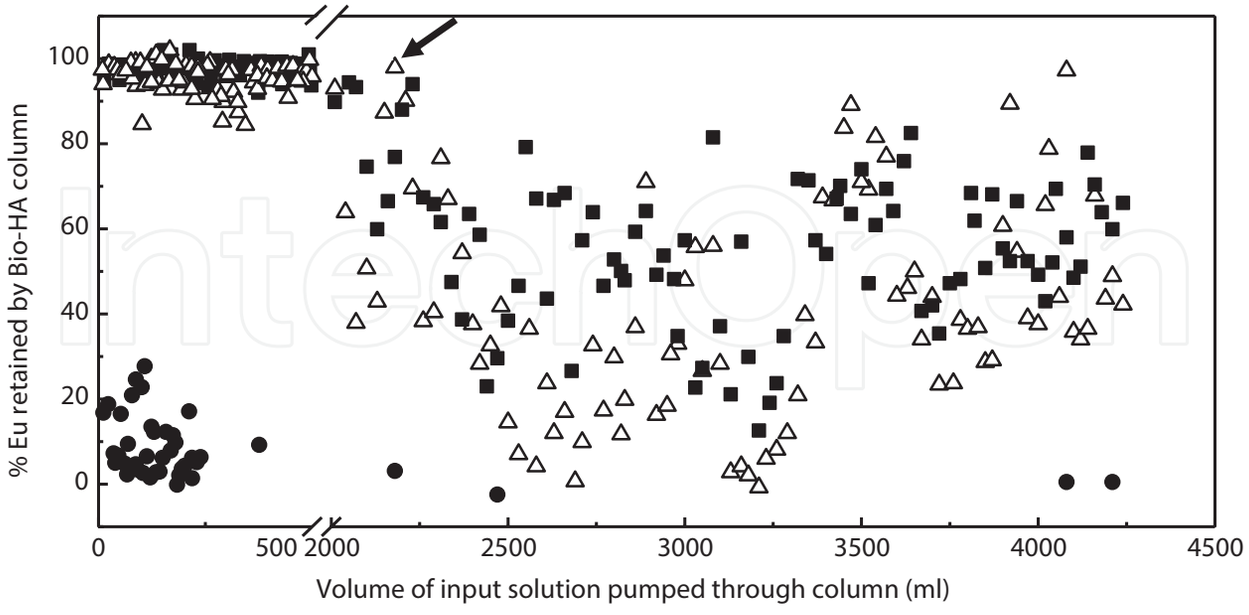


Figure 11. Uptake of Eu^{3+} by bacterial HA. The setup was shown in Figure 2 except that the loading solution was 1 mM Ca^{2+}, 5 mM glycerol 2-phosphate and 2 mM citrate buffered to pH 9.2 (25 mM TAPSO) for the loading of hydroxyapatite. The columns from independent biofilm preparations I and II (■, △) were drained, and the flow changed to 0.5 mM $Eu(NO_3)_3$ (aq). Column exit solution was assayed for Eu^{3+} colorimetrically; selected samples were retained for analysis of Eu, P and Ca by inductively coupled plasma optical emission spectroscopy (ICP-OES) in Table 3. ●: control (biofilm only). Arrow: Eu^{3+} breakthrough.

Volume passed (L)	Eu^{3+} accumulated (mmol/L)	Ca^{2+} evolved (mmol/L)	Pi evolved (mmol/L)
0–2	0.47 ± 0.04	0.56 ± 0.31	0.28 ± 0.02 (0-0.6 L)
			0.10 ± 0.02 (0.6–2 L)
2–4	0.22 ± 0.03	0.23 ± 0.01	0.017± 0.003 (2–4 L)

Table 3. Eu^{3+} uptake into immobilised bio-HA and Ca^{2+} and phosphate (Pi) evolved.

Since the column was not saturated with Eu^{3+} by the 4 L stage, this study suggests that a surface layer of bio-HA was initially saturated and then a second phase occurred whereby incoming Eu^{3+} exchanged for Ca^{2+} in deeper layers of the HA-biofilm in a slower process. The variation of Eu^{3+} removal in the second stage ranged from 0 to 100% which possibly reflects discontinuous access of new parts of the bio-HA as the column becomes saturated in the readily accessible areas. **Figure 9C** and **D** suggests that the bio-HA is not homogeneous in the biofilm. While magnetic resonance imaging (MRI) has been applied to visualise biofilms in the foam *in situ* and also during HA-loading [70] and could be used to monitor progressive ingress of the paramagnetic REE^{3+} species (Gd is a well-known contrast agent in MRI due to its paramagnetic effect) as described for mapping of paramagnetic Cr(VI) in columns [80]. The resolution of MRI (~100 μm) is insufficient to visualise even the detail of the foam struts and the biofilm appeared as an indistinct layer on them [70]; hence spatial analysis of the Eu^{3+} penetration into the bio-HA would be very difficult, additionally because of the long image acquisition times required. More extensive work is required to optimise the bio-HA loading on the biofilm and to obtain a more even distribution. It may also be found useful to use a fluidised bed delivery to ensure more even penetration throughout all exposed surfaces and to avoid channelling behaviour within the column.

Although bio-HA was found to take up both Eu^{3+} and UO_2^{2+} separately, the failure of the former in commercial HA only (**Table 2**) and the ability of the bio-material to take up Sr^{2+} from seawater (high saline) where commercial HA cannot [19] suggest bio-HA to be a new bio-agent for REE recovery. However, experiments using metal mixtures in realistic matrix backgrounds are needed in order to evaluate the scope for metal selectivity in actual applications. To aid further studies, insight into the structure of the bio-material is required.

11. Structure of bio-HA and mechanism of REE sequestration

The above discussions suggest that bio-HA differs in some way from its chemical counterpart. It is important to note that XRD analysis examines bulk sample and reports on only those components that are crystalline (even if in minor amounts), while selected area electron diffraction analysis examines only very small spots within a sample. The broad peaks for bio-HA [74, 78, 79] suggest the material contains poorly crystalline or amorphous components, as confirmed by the analysis of its crystallinity (below).

A detailed investigation was made of calcium phosphates made chemically in a groundwater matrix with and without added bacteria [81]. Ground waters contain the naturally occurring

geopolymers, humic and fulvic acids and, with bacteria, organic acids derived from bacterial metabolism and also microbial extracellular polymers.

The mineral progressed from the initial formation of amorphous calcium phosphate and transformation to poorly crystalline HA within 7 days. The presence of bacteria delayed the onset of precipitation, resulted in changes to the lattice parameters and also reduced incorporation of trace elements as compared to cell-free systems. Importantly, that study [81] distinguishes between the ability of HA to form in a passive, bacterially supplemented system (with added external phosphate) [81], as compared to one in which the phosphate is being supplied enzymatically within the extracellular polymeric matrix [the *Serratia* example system described in this work]; both indicate that the matrix with/of the bacteria influences the formation of HA, its lattice structure and also its ability to take up secondary metals. A detailed discussion is outside the scope of this chapter (see [81]) but salient points highlighted were the effect of organic compounds with respect to HA crystallinity, also noting that uptake of Sr^{2+} into HA decreased in the presence of bacteria during HA synthesis (the uptake of Sr^{2+} into pre-formed HA was not tested). Specifically, it was cited that the presence of citrate (relative to acetate) in the mixture had the effect of decreasing the crystal size and showed both a higher content of impurities and a higher incorporation of carboxylate groups into the crystal structure [82]. We suggest that by fabricating the HA from within the EPM (**Figure 9A**), fed by enzymatically generated phosphate, a novel scaffolded HA is formed, with crystal growth controlled by the surrounding EPM-matrix, which may promote features enabling it to take up Eu^{3+} efficiently even after heating (i.e. a persistent matrix 'memory') whereas 'chemical HA' would lack this property (**Table 2**).

An early analysis of bio-HA made under the conditions described here (**Figures 10** and **11**; **Table 3**) confirmed formation of a hydroxyapatite material that converted to β-tricalcium phosphate (β-TCP) after sintering [83]. Further analysis [84] showed that non-sintered material comprised mainly calcium-deficient HA (CDHA) of ~9% crystallinity which increased to 53% after sintering at 1200°C, with the sintered material identified by X-ray diffraction and Fourier Transform Infrared spectroscopy as mainly CDHA with some sodium calcium phosphate. In the bio-HA (native, treated at 600°C and sintered at 1200°C) the stretching O-H bond (characteristic of the commercial HA spectrum at wavenumber 3566 cm^{-1}) was absent, suggesting that the HA crystal lattice is defective; Ledo et al. [84] discussed the possible presence of vacant calcium sites and hydroxide ion sites and/or that some of the phosphate ions may be either protonated or substituted by other ions. They also suggested that the EPM materials were associated with the bio-HA and were destroyed upon sintering. Thackray et al. [83] suggested that after sintering bio-HA comprised β-tricalcium phosphate as a dominant phase, together with small amounts of $Na_3Ca_6(PO_4)_5$ and $NaCaPO_4$. The Na^+ ions probably arise from the sodium salt of G2P used in bio-HA synthesis. They also noted that the presence of impurities may influence the phase composition, the final material after sintering reflecting the method used to produce it. Formation of CDHA or β-TCP after sintering depended on the initial Ca:P ratio, while crystals produced at pH 9.2 in the presence of citrate remained as HA while those produced at pH 8.6 without citrate sintered to β-TCP [84]. As bulk production of bio-HA would probably require heat treatment to remove both bacterial cells and pyrogens, these differences may impact upon the properties with respect to the subsequent REE uptake.

HA materials are polycrystalline with characteristic grain boundaries containing amorphous calcium phosphate species; the highly amorphous nature of bio-HA together with the high occurrence of organic materials (above) suggests that the occurrence of grain boundaries would be large but it is difficult to see how Eu^{3+} was loaded to >80% of the HA mineral weight [78] unless most of the material comprised ultra-small crystallites with a high proportion of surface calcium phosphate groups as compared to buried ones. It would be possible to calculate this in homogeneous material of known crystallite size but the nature of bio-HA and dependence on the exact conditions of synthesis would make this calculation very difficult.

In HA, 10 calcium atoms are aligned in two non-equivalent sites denoted as Ca(I) and Ca(II). It was reported that these sites are the target for divalent cation substitution [85] but the evidence for trivalent REE binding is less clear. Two studies had reported the incorporation of Eu^{3+} into the Ca(I) sites of apatite at room temperature via use of time-resolved laser fluorescence spectroscopy (TRLFS) (see [72]) but in contrast the trivalent actinide Cm^{3+} incorporated into the apatite mineral structure [72]. Holliday et al. [72] used TRLFS in conjunction with extended X-ray absorption fine structure (EXAFS) to eliminate the Ca(I) site as the target for Eu^{3+} incorporation, pointing out that poorly defined Eu^{3+} would exist in an amorphous environment with both the fluorescence lifetime and emission spectra indicating that Eu^{3+} does not incorporate into the HA crystal structure but with the excitation spectrum showing a broad peak that would be expected by location of Eu^{3+} in an amorphous environment [72]. Persistent biological residue was largely discounted since biologically produced and synthetic apatite gave identical fluorescence emission spectra; moreover, even after sintering to remove biological material only ~50% loss of crystallinity was achieved [83] i.e. a largely amorphous material with very small crystallites. Holliday et al. [72] concluded that Eu^{3+} incorporates into grain boundaries and not Ca(I) or Ca(II) sites.

β-TCP is a known feature of grain boundaries in bio-HA [83] (above) but TCP results from bio-HA after heat treatment whereas native material was used by Holliday et al. [72]. Hence, the data appear inconsistent, especially given the high loadings of Eu^{3+} observed into bio-HA in several independent studies [73, 78, 79] and since only a low uptake of Eu^{3+} was seen using commercial HA (**Table 2**), in accordance with a hypothesis that suggests non-penetration into the Ca(I) and Ca(II) sites of the crystalline material. Handley-Sidhu et al. [73] argued that removal of the organic material by heating left voids and hence a large number of grain boundaries for Eu^{3+} uptake and they also noted that there was no change in the XRD pattern after Eu-substitution, suggesting no incorporation into the mineral mass. However, XRD only provides information on the crystalline components, not the amorphous material, and, even after sintering, ~half of the bio-material remained amorphous [83].

The bi-phasic nature of the Eu^{3+} uptake into bio-HA (**Figure 11**), the high capacity (**Figure 10**) and the clear stoichiometry of Eu^{3+} uptake and Ca^{2+} release (**Table 3**) clearly argue for two mechanisms: an initial saturation of grain boundary sites (patterned by the original organic matrix) followed by a slower uptake via ion exchange. Inspection of three studies shows that Holliday et al. [72] used only 1 μM Eu^{3+} whereas Gangappa et al. [78] and Handley-Sidhu et al. [73] used 0.5 and 10 mM Eu^{3+}, respectively. It is likely that the Eu^{3+} in the former study [72] was sufficient only to bind (preferentially) to surface sites whereas a higher concentration of

Eu^{3+} allowed, over time, a bypass or migration of the surface-bound Eu^{3+} to deeper locations, resulting in a slower uptake phase with, presumably, migration of the surface located Eu^{3+} into deeper layers being rate-limiting. This was indirectly supported by the observation that it was difficult to describe metal uptake into bio-HA by classical Langmuir or Freundlich isotherm analysis [19]. If so, then the architecture of the surface of the HA is a key to the subsequent uptake and incorporation reactions giving >80% saturation of the HA. In a batch suspension this required ~24 h for completion [79] (**Figure 10**) whereas with the column study (using grams of HA material and a continuous Eu^{3+} feed: **Figure 11**) saturation of the first uptake phase occurred after 125 column volumes (250 h) but that of the second (ion exchange only: **Table 3**) was not seen even after 250 column volumes (500 h).

As described above, the presence of organic materials can impact upon the nano-crystalline format and maintains a large number of grain boundaries for the surface interactions but it is now becoming appreciated that organic ligands in the matrix (whether from the suspension or from the bio-matrix itself) also impact upon the actual surface structure (see earlier discussions). In parallel work, the presence of organic ligands from wastes was used in the background matrix during HA synthesis [18]. By this approach the uptake of Cu(II) into HA was increased by several-fold as compared to chemical HA made without chemical ligands, to 850 mg Cu/g HA (85% of the mass) [18]. However, when corrected for the different atomic masses of Cu and Eu the uptake of metal into the bio-HA (this study) was >2-fold higher than for the material made with applied ligands [18]. The extent to which the very high substitution of Eu^{3+} may destabilise the bio-HA lattice is not known but the lack of inorganic phosphate recovered (**Table 3**) suggests that the composite material is stable. A detailed study of its structure is underway.

12. Potential for selective REE recovery: applications of a magnetic field

Initial tests used the biofilm (enzymatic) system on columns challenged with either Nd^{3+} or Eu^{3+} with the columns positioned between external Nd permanent magnets in the enzymatic bio-mineralisation mode. The different magnetic properties of the REE [86] might be expected to enrich for the more magnetically active element(s) in the biofilm at the bottom of the column. However, with both Nd^{3+} and Eu^{3+} (separately) the columns rapidly lost activity. The reason for this was not investigated but it is likely that a metallic co-factor (e.g. Fe or Mn) was stripped from the enzyme; the role of Fe in the function of purple acid phosphatases (for example) is well known [87]. Hence, a magnetic separation would not be possible using the enzymatic recovery route and the ion exchange route into bio-HA is more attractive. Nd^{3+} and Eu^{3+} were loaded (separately) into bio-HA as described above and the material was squeezed from the biofilm-HA discs. While bio-HA alone gave no response, REE-substituted HA was collected rapidly onto the magnet [88]. The migration rates of Nd-HA and Eu-HA were not measured but the potential for magnetic separation using a bio-HA 'collector' in a magnetic field would be worthy of further exploration as a means for possible REE enrichment. A column system is non-ideal but future tests would envisage a fluidised bed held in a magnetic gradient; appropriate systems for separation of differentially magnetised-HA are under current investigation.

13. Potential for selective REE recovery: a biotechnology approach

Previous work has shown that pre-nucleation enhanced $NdPO_4$ deposition in aged biofilms [89]. This expanded from early work showing that pre-nucleation by one metal phosphate could promote the subsequent recovery of a different 'target' metal [29].

As part of the TBP study (above; S. Moriyama, I. Mikheenko and L.E. Macaskie, unpublished) (using 1 mM G2P/2 mM TBP and 1 mM metal ion in 2 mM citrate) the removal of uranyl ion by a column pre-nucleated with uranyl phosphate deposit (at the $FA_{1/2}$ value for removal of Nd^{3+} in the single metal flows) was less than 10%. Conversely, a column that had been pre-nucleated with $NdPO_4$ from the same background mixture gave enhanced removal of uranyl ion (35%) at the same flow rate. In contrast, pre-nucleation with uranyl phosphate followed by challenge with Nd^{3+} gave only 18% removal of Nd^{3+}, not 50% as in the single metal tests (although the pre-loading extents of $NdPO_4$ and HUO_2PO_4 were not the same). This suggests that, while a nucleation deposit of $NdPO_4$ may assist in the recovery of uranyl ion, the converse is true for neodymium recovery. This concept of a 'keying' (or indeed blocking) metal deposit laid down in advance of the REE mixture of interest suggested a possible development of this pre-nucleation concept towards selective recovery of REE. An initial survey [90] used suspended cells of 25 bacterial species expressing various levels of phosphatase activity. A selection of metals/bio-minerals was pre-deposited onto the cells prior to exposure to REE^{3+}. These initial metal deposits (low cost metals of low toxicity) were designated as 'Keying Metal A-Z.' With a high number of combinations, a column test in each case was impractical and these tests used batch suspensions. Selected examples are shown in **Figure 12**.

Figure 12A shows a strain pre-treated with three different 'keying' materials. Recovery of the REE was ~15–25% (mol/mol of the starting amount) but with little selectivity between them. Although Lu was rejected (i.e. enriched in the residual solution) negligible enhancement of REE removal was observed using three 'keying metals'. In contrast (**Figure 12B**) strain 17B when 'keyed' with material Z showed some selectivity. Native and 'keyed' cells rejected Lu^{3+} and Gd^{3+} (**Figure 12B**) and the 'keying' procedure increased the rejection of La^{3+} and Pr^{3+}. Selectivity was shown for the light REEs by up to 2-fold.

The rejection of La^{3+} and Pr^{3+} implies a competition between these and the 'keying' metal for deposition sites. Metal uptake in this set of experiments was not via phosphatase activity (no phosphate donor was provided) and a metal uptake mechanism akin to REE uptake into pre-mineralised cells (above) or via ion exchange (as with bio-HA) is implied or, indeed, metal diversion and uptake onto other bacterial surface sites following blockage of preferred in the 'keying' step. Analysis for keying metal appearing in solution and mass balances (e.g. as in **Table 2**) has not been attempted and would form the focus of future work.

Bio-sorption of metals onto functional groups of microbial cells is very well documented since the 1980s [91] and is now enjoying a resurgence as the price of metals rises (as well as environmental concerns about the impact of primary resource extraction), via a new generation of researchers (e.g. [92]). It is known which biological ligand group favours a particular

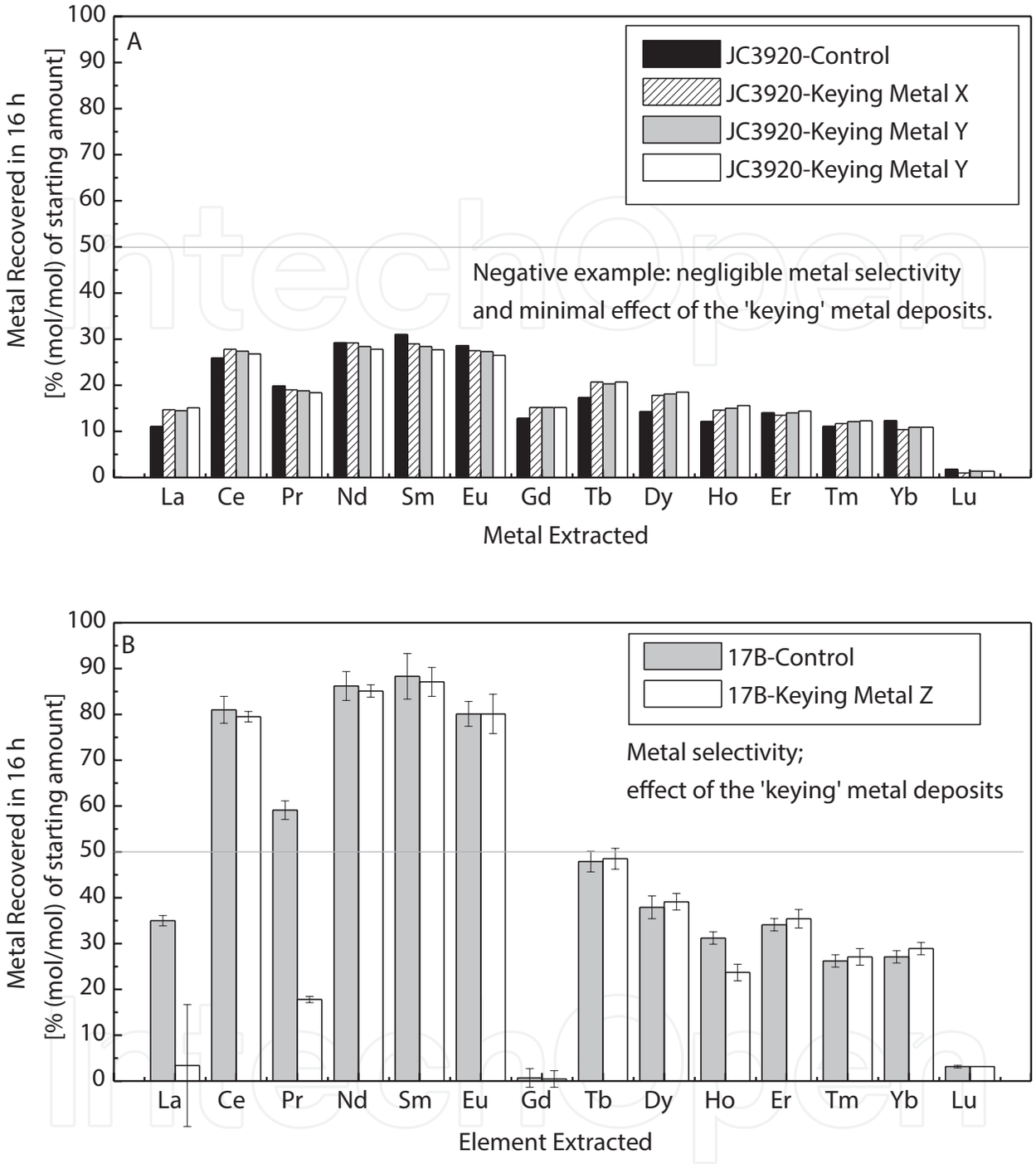


Figure 12. Effect of 'keying' bacteria with another metal deposit prior to exposure to metal of interest. In all experiments, equimolar amounts (approximately 1 mM in all cases, assessed by clean-room ICP-MS) of La-Lu as REE^{3+} chlorides were added as a mixture to bio-recovery medium (buffered to pH 7.2, $CaCl_2$, G2P and glycerol) from individual stock solutions immediately after supplementing with pre-grown, active cells of the bio-recovery organism under test (final volume 50 mL). After 16 h exposure at 22°C with gentle agitation, cells were harvested by filtration and washed thoroughly with deionised water to remove unbound metals before digestion in hot brominated *aqua regia* to degrade the biomass. Biomass-associated REE were analysed in the digestate by clean-room ICP-MS. Cells were also pre-treated with the 'keying' metals by a proprietary method. All data shown are expressed as % (mol/mol) recovery of metal from solution; error bars are standard error of the mean (N = 3). Reproduced from Ref. [90] with permission. (A) shows an example where there is no metal selectivity with keying deposit (strain JC920). (B) shows an example of metal selectivity using strain 17B with 'keying metal' deposit.

metal but the concept of metal-organic frameworks (MOFs; see earlier) with respect to the role of bacterial cell surfaces as potential MOFs is almost unexplored. In the current example (**Figure 12B**) it is possible that the second metal inserts into an extant MOF on the bacteria, which may be unique for each bacterial species (and also their specific growth conditions) and metal combination(s) as well as other ligands in the solution matrix, and the pH. The preliminary study made by Boden et al. (**Figure 12**) informs, by the use of known 'blocking', a future combinatorial chemistry and synthetic biology approach, given the large number of REE and relatively recent focus on their chemistry.

14. Future outlook

For process application the *Serratia* enzymatic method was initially proposed to provide a rapid and efficient way to achieve non-specific REE accumulation against uranyl ion into a mineral concentrate. However, this over-simplistic projection does not take into account the possible formation of metal organic frameworks in microbial EPM and the external solution in a bimetallic system that could 'push' a readily available metal into a less-available form. The use of TBP is shown to be of no benefit in the separation of REE and uranium, serving only to reduce metal recovery overall. Clearly an enzymatic route to metal recovery from real wastes may have limitations where metal separation is required, although this approach was highly effective in a uranium-only system [33, 47] and in the separation of REE(III) and Th(IV) by the restriction of flow residence time (**Figure 3**).

A study of HA formation by the same bacteria showed extensive deposition and, in this sense, the initial complexation of the Ca^{2+} into the bacterial exopolymer could be taken as an example of a simplistic, single metal MOF in the initial stages of bio-HA deposition. This concept of selectivity of metals into natural matrices to provide nucleation or 'keying' deposits to assist in the selective recovery of a second metal is a step change, inspired by observational studies, that now requires the concerted applications of combinatorial chemistry and synthetic biology to achieve further advances in targeted REE recovery, where the nature of the bacterial EPM or other bacterial surface layers provides a potential tool for manipulation using synthetic biology approaches.

Commercial implementation would assume no current selectivity of REE recovery and initially would aim to obtain a bulk metal phosphate bio-mineral for onward refining or prior to making a more concentrated leachate for a secondary selective REE recovery (possibly an ammonium sulphate leach, then a second, alkaline stage using bi-carbonate ion) but the overall economics is key. The possibility to provide a uranium concentrate as a high value side stream would be important. Within a previous EU consortium project [47], the cost of the *Serratia* bio-recovery process was estimated as comparable to ion exchange in terms of capital outlay but operational cost (the need for G2P for continued metal synthesis) was limiting and TBP is concluded to have little potential for realistic substitution for G2P due to complexities of the bio-chemistry of its utilisation. A similar conclusion regarding alkyl phosphate utility was reported elsewhere (see [81]).

In contrast to the high current commodity value of REE, uranium was of little importance in 1990s when the uranium recovery study was done [33, 47] (US$ 10/lb) but, with a global nuclear expansion, in response to concern about fossil fuel availability and the environmental consequences of CO_2 emissions, the economic and environmental impacts of a dual metal recovery become compelling.

With respect to the bacteria required for metal recovery, custom-growing of bacteria is costly. However, waste could be used, for example by pre-growing the bacteria on lactose (e.g. dairy waste) and ammonium phosphate (e.g. fertiliser) [47]. In terms of metal recovered against 'biomass elemental building blocks' (C, N, S, P), at a metal loading of 5–10 times the bacterial dry weight (reported for bio-mineralisation within columns) the 'building blocks' would account for a small proportion of the total solid upon ashing for delivery into current pyro- and hydro-metallurgies and bio-recovery represents a mechanism to convert large volumes of dilute metals into solid concentrates.

The high value of REE, and difficulty of their extraction by conventional methods, suggests a potentially cost-effective process, especially if the 'bulk recovery' *Serratia* column can be re-used. A secondary selective step from leachates from the *Serratia* column will require future synthetic biology developments for bio-material engineering towards REE selectivity but the feasibility is shown in **Figure 12B** and below.

To overcome the economic bottleneck of bulk phosphate supply, phytic acid, a plant storage material (a waste from bio-diesel production from plant materials), was shown to be cleaved enzymatically to support metal removal [93] although the low water-solubility of phytic acid (inositol phosphate) may pose operational difficulties.

In a worst-case scenario, where REE recovery from the *Serratia* column via leaching into a concentrate for a selective secondary REE recovery is not achieved, the fall-back option would be delivery of a concentrated solid into commercial refining. Since a large proportion of the cost of ore and waste solids processing involves comminution (a large energy demand and hence high environmental CO_2 burden) microbial generation of nano-phase concentrated materials for recycling would represent energy savings (less comminution of finely divided material) as well as waste volume reductions and hence transportation and handling costs. This process intensification (as well as various Life Cycle Analyses) is the current status of the biotechnology approach to REE bio-refining, and this chapter highlights the future potential and currently identified bottlenecks, as well as the large scope for both combinatorial chemistry and synthetic biology as combined tools. In this respect, 'biosorption' of metals has 'come of age' in that a vast literature of biosorption studies exists over the past 50 years for many types of microorganism, bio-polymers and metals/metal combinations and the use of data mining and *in silico* methods may prove essential to inform and shorten the delivery of combinatorial chemistry and synthetic biology approaches.

Following early studies on the use of selective metal binding peptides and proteins on cells [94, 95], two recent studies highlight this potential. An acidophilic fungal isolate (a *Penidella* sp.) accumulated dysprosium and other REEs to 0.9 mg/g dry biomass (9% of the biomass dry weight) [96], while a strain of the stalked, biofilm-forming bacterium *Caulobacter crescentus*

was engineered to display lanthanide binding tags on the cell surface, endowing specificity for some REEs over others and selectivity against Ca^{2+} [4]. The 'tags' were attached to the protein S-layer surrounding the cells. The sorption of Tb^{3+} was stated [4] as 50 μM at a cell concentration of 8×10^8 cells/mL (i.e. assuming the mass of a single cell as 1 pg, an uptake of approximately 1% of the bacterial dry weight, comparing favourably with other biosorption systems) but it was not stated whether the cells were saturated with Tb. A low capacity is acceptable if the sorbent can be re-used; the REEs could be eluted using citrate in sequential sorption/elution cycles [4]. A mixed REE test solution was made from an *aqua regia* extract of an environmental sample (125°C; 8 h), hence the background organic matrix would have been modified before use during tests. Thermodynamic modelling was done according to established models (from 2002 to 2006 [4]) for a solution of Tb, Ce, citrates and acetates to assess the likely speciation of Tb^{3+} but the potential contributions of additional metals and, indeed, potential MOFs in real samples, would be important to establish in progression to real life application.

Acknowledgements

The authors acknowledge with thanks the support of NERC (Grant NE/L014076/1) and EPSRC (EP/M012719/1 supporting joint UK-Japan civil nuclear research) and the collaboration of The University of Plymouth, UK: Dr Rich Boden who obtained the data shown in **Figure 12** (taken from [90] with permission; A.J. Murray et al., senior author L.E. Macaskie; printed in 'Proceedings COM 2014 International Conference, Hyatt Regency Hotel, Vancouver Sept 28-Oct 1, 2014'). They wish to thank Drs R. Clough for help in ICP-OES analysis and S. Ward, without whom essential data could not have been obtained. **Figure 4** is reproduced from [16] with permission from the Royal Society of Chemistry, while **Figure 7** has been re-drawn from data presented in reference [57]. We also thank Drs P. Yong and M. Paterson-Beedle for use of unpublished information and Dr J.A. Hriljac (School of Chemistry, University of Birmingham) for helpful discussions.

Author details

Lynne E. Macaskie*, Sayo Moriyama, Iryna Mikheenko, Sarah Singh and Angela J. Murray

*Address all correspondence to: l.e.macaskie@bham.ac.uk

School of Biosciences, University of Birmingham, Edgbaston, Birmingham, UK

References

[1] Anon. Development of a Sustainable Exploitation Scheme for Europe's Rare Earth Deposits. http://www.eurare.eu. [Accessed 30-01-2017]

[2] Sun X, Waters KE. Development of industrial extractants into functional ionic liquids for environmentally friendly rare earth element separation. ACS Sustainable Chemistry and Engineering. 2014;**2**:1910-1917. DOI: 10.1021/sc500255n

[3] Zhang MM, Li HX, Andrade M, Xuan W, Correa A. Feasible bioprocessing technologies for low grade iron ores al. Minerals and Metallurgical Processing Journal. 2015;**32**:78-87

[4] Park DM, Reed DW, Yung M, Elsamimanesh A, Lencka MM, Anderko A, Fujita Y, Riman RE, Navrotsky A, Jiao Y. Bioadsorption of rare earth elements through cell surface display of lanthanide binding tags. Environmental Science and Technology. 2016;**50**:2735-2742. DOI: 10.1021/acs.est.5b06129

[5] Moriwaki H, Yamamoto H. Interactions of microorganisms with rare earth ions and their utilization for separation and environmental technology. Applied Microbiology and Biotechnology. 2013;**97**:1-8. DOI: 10.1007/s00253-012-4519-9

[6] Ozaki T, Suzuki Y, Yoshida T, Ohnuki T, Nankawa T, Francis AJ. Association of Eu(III) with bacteria and organic ligands. Journal of Nuclear and Radiochemical Science. 2005;**6**:73-76

[7] Takahashi T, Chatellier X, Hattori KH, Kato K, Fortin D. Adsorption of rare earth elements onto bacterial cell walls and its implications for rare earth sorption onto natural microbial mats. Chemical Geology. 2005;**219**:53-67. DOI: 10.1016/j.chemgeo.2005.02.009

[8] Takahashi Y, Yamamoto M, Yamamoto Y, Tanaka K. EXAFS study on the cause of enrichment of heavy rare earths on bacterial cell surfaces. Geochimica et Cosmochimica Acta. 2010;**74**:5443-5462. DOI: 10.1016/j.gca.2010.07.001

[9] Jiang M, Ohnuki T, Tanaka K, Kozai N, Kamiishi K, Utsunomiya S. Post-adsorption process of Yb phosphate nanoparticle formation by *Saccharomyces cerevisiae*. Geochimica et Cosmochimica Acta. 2012;**93**:30-46. DOI: 10.1016/j.gca.2012.06.016

[10] Gadd GM. Metals, minerals and microbes: Geomicrobiology and bioremediation. Microbiology. 2010;**156**:609-643. DOI: 10.1099/mic.0.037143-0

[11] Van der Watt JG, Wanders FB. Leaching of rare earth elements from bentonite clay. Journal of South African Institute of Mining and Metallurgy. 2012;**112**:273-285

[12] Goyne KW, Brantley SL, Chorver J. Rare earth element release from phosphate minerals in the presence of organic acids. Chemical Geology. 2010;**278**:1-14. DOI: 10.1016/j.chemgeo.2010.03.011

[13] Shan X, Lian J, Wen B. Effect of organic acids on adsorption and desorption of rare earth elements. Chemosphere. 2002;**47**:701-710. DOI: 10.1016/S0045-6535(02)00032-2

[14] Nockermann P, Thijs B, Parac-Vogt TN, Hecke KV, Meervelt LV. Tinant B, Hartenbach I, Schleid T, Nguyen MT, Binnemans K. Carboxyl-functionalized task-specific ionic liquids for solubilizing metal oxides. Inorganic Chemistry. 2008;**47**:9987-9999. DOI: 10.1021/ic801213z

[15] Mann S. Biomineralization: Principles and Concepts in Bioinorganic Materials Chemistry. Oxford: Oxford University Press; 2001. pp. 210

[16] Nelson YM, Lion LW, Ghiorse WC, Shuler ML. Production of biogenic manganese oxides by *Leptothrix discophora* SS-1 in a chemically defined medium and evaluation of their Pb adsorption characteristics. Applied and Environmental Microbiology. 1999;**65**:175-180

[17] Nelson YM, Lion LW, Shuker ML, Ghiorse WC. Effect of oxide formation mechanisms on lead adsorption by biogenic manganese (hydr) oxides and their mixtures. Environmental Science and Technology. 2002;**36**:421-425. DOI: 10.1021/es010907c

[18] Mercardo DF, Magnacca G, Malandrino M, Rubert AA, Montoneri E, Celi L, Prevot AB. Gonzalez MC. Paramagnetic iron-doped hydroxyapatite nanoparticles with improved metal sorption properties. A Bio-organic substrates-mediated synthesis. ACS Applied Materials and Interfaces. 2014;**6**:3937-3946. DOI: 10.1021/am405217j

[19] Handley-Sidhu S, Mullan S, Grail Q, Albadarneh M, Ohnuki T, Macaskie LE. Influence of pH, competitor ions and salinity on the sorption of strontium and cobalt onto biogenic hydroxyapatite. Scientific Reports. 2016. Article No 23361. DOI: 10.1038/srep23361

[20] Tolley MR, Strachan LF, Macaskie LE. Lanthanum accumulation from acidic solutions using a *Citrobacter* sp. immobilized in a flow through bioreactor. Journal of Industrial Microbiology. 1995;**14**:271-280. DOI: 10.1007/BF01569939

[21] Murray AJ, Singh S, Vavlekas D, Tolley MR, Macaskie LE. Continuous biocatalytic recovery of neodymium and europium. RSC Advances. 2015;**5**:8496-8506. DOI: 10.1039/C4RA14892D

[22] Murray AJ, Singh S, Vavlekas D, Tolley MR, Macaskie LE. Biorecovery of rare earth elements: potential application for mine water remediation. Advanced Materials Research. 2015;**1130**:543-547. DOI: 10.4028/www.scientific.net/AMR.1130.543

[23] Friebe N, Nuyken O, Obrecht W. Neodymium-based Ziegler-Natta catalysts and their application in diene polymerization In: Nuyken O, editor. Neodymium-based Zeigler Catalysts Fundamental Chemistry. Berlin: Springer-Verlag; 2006. pp. 1-154. DOI: 10.1007/12_094

[24] Chen F, Zhu Y-J, Zhang K-H, Wu J, Wang K-W, Tang Q-L, Mo X-M. Europium-doped amorphous calcium phosphate porous nanospheres: Preparation and application as luminescent drug carriers. Nanoscale Research Letters. 2011;**6**:67-76. DOI: 10.1186/1556-276X-6-67

[25] Pisarska J, Soltys M, Zur L, Pisarski WA, Jayasankar CK. Excitation and luminescence of rare earth-doped lead phosphate glasses. Applied Physics B. 2014;**116**:837-845. DOI: 10.1007/s00340-014-5770-9

[26] Macaskie LE, Mikheenko IP, Yong P, Deplanche K, Murray AJ, Paterson-Beedle M, Coker VS, Pearce CI, Cutting R, Pattrick RAD, Vaughan D, Van Der Laan G, Lloyd JR. Today's wastes tomorrow's materials for environmental protection. In: Moo-Young M,

Butler M, Webb C, Moreira A, Grodzinski B, Cui ZF, Agathos S, editors. Comprehensive Biotechnology. Amsterdam Elsevier. 2011;**6**:719-725

[27] Jeong BC, Hawes C, Bonthrone KM, Macaskie LE. Localisation of enzymically enhanced heavy metal accumulation by a *Citrobacter* sp. and metal accumulation in vitro by liposomes containing entrapped enzyme. Microbiology. 1997:**143**:2497-2507. DOI: 10.1099/00221287-143-7-2497

[28] Macaskie LE, Jeong BC, Tolley MR. Enzymatically accelerated biomineralization of heavy metals-application to the removal of americium and plutonium from aqueous flows. FEMS Microbiology Reviews. 1994;**14**:351-367. DOI: 10.1111/j.1574-6976.1994.tb00109.x

[29] Macaskie LE, Lloyd JR, Thomas RAP, Tolley MR. The use of microorganisms for the remediation of solutions contaminated with actinide elements, other radionuclides and organic contaminants generated by nuclear fuel cycle activities. Nuclear Energy. 1996;**35**:257-271

[30] Macaskie LE, Empson RM, Lin F, Tolley MR. Enzymatically-mediated uranium accumulation and uranium recovery using a *Citrobacter* sp. Immobilized as a biofilm within a plug-flow reactor. Journal of Chemical Technology and Biotechnology. 1995;**63**:1-16. DOI: 10.1002/jctb.280630102

[31] Petit LD, Powell KJ. Stability Constants Database. UK: SC-Database IUPAC and Academic Software; 2008

[32] Jeong BC, Kim HW, Macaskie LE. Phosphotransferase activity of acid phosphatases of a *Citrobacter* sp. Federation of European Microbiological Societies Microbiology Letters.1997;**147**:103-108. DOI: 10.1111/j.1574-6968.1997.tb10227.x

[33] Macaskie LE, Yong P, Doyle TC, Manzano TM, Roig M. Bioremediation of uranium-waste: biochemical and chemical factors affecting bioprocess application. Biotechnology and Bioengineering. 1997;**53**:100-109. DOI: 10.1002/(SICI)1097-0290(19970105)53:1<100::AID-BIT13>3.0.CO;2

[34] Yong P, Macaskie LE. The role of sulfate as a competitive inhibitor of enzymatically mediated heavy metal uptake by *Citrobacter* sp: Implications in the bioremediation of acid mine drainage water using biogenic phosphate precipitant. Journal of Chemical Technology and Biotechnology. 1999;**74**:1149-1156. DOI: 10.1002/(SICI)1097-4660(199912)74:12<1149::AID-JCTB164>3.0.CO;2-0

[35] Yong P, Macaskie LE. The effect of substrate concentration and nitrate inhibition on phosphate release and heavy metal removal by a *Citrobacter* sp. Biotechnology and Bioengineering, 1997;**55**:821-830. DOI: 10.1002/(SICI)1097-0290(19970920)55:6<821::AID-BIT1>3.0.CO;2-I

[36] Vavlekas DA. Construction and evaluation of a modular biofilm-forming chamber for microbial recovery of neodymium and semi-continuous biofilm preparation. Tolerance of *Serratia* sp.N14 on acidic conditions and neutralized *aqua regia*. Environmental Technology. 2016;**38**:1-18. DOI: 10.1080/09593330.2016.1189971

[37] Jeong BC. Studies on the atypical phosphatase of a metal accumulating *Citrobacter* sp. [D.Phil Thesis]. UK University of Oxford; 1992.

[38] Jambor JL, Roberts AC, Owens DR, Grice JD. Zajacite-(Ce) a new rare earth fluoride from the Strange Lake deposit, Quebec, Labrador. Canadian Mineralogist. 1996;**34**:1299-1304. http://rruff.info/doclib/cm/vol34/CM34_1299.pdf

[39] Anon (May, 2016) http://www.marketwired.com/press-release/pele-mountain-provides-update-on-development-plans-and-progress-in-elliot-lake-tsx-venture-gem-2121413.htm [Accessed 10-12-2016]

[40] Tolley MR. The Biological Treatment of Liquid Wastes Containing heavy metals [D. Phil Thesis]. UK University of Oxford; 1993.

[41] Paterson-Beedle M, Macaskie LE, Lee CH, Hriljac JA, Jee KY, Kim WH. Utilization of hydrogen uranyl phosphate based ion exchanger supported on biofilm for the removal of cobalt, strontium and caesium from aqueous solutions. Hydrometallurgy. 2006;**83**:141-145. DOI: 10.1016/j.hydromet.2006.03.020

[42] Ohnuki T, Kozai N, Sakamoto F, Suzuki Y, Yoshida T. Biological change of chemical states of actinides and lanthanides—effects of organic acids. Energy Procedia. 2013;**39**:175-183. DOI: 10.1016/j.egypro.2013.07.204

[43] Amico P, Daniele PG, Ostacoli G, Sammartano S. Mixed metal complexes in solution Part 4. Formation and stability of heterobinuclear complexes of cadmium II-citrate with some bivalent metal ions in aqueous solution. Transition Metal Chemistry. 1985;**10**:11-14. DOI: 10.1007/BF00620623

[44] Raju U, Warker SG, Kumar A. Green synthesis of multi-metal-citrate complexes and their characterization. Journal of Molecular Structure. 2017:**1133**:90-94. DOI: 10.1016/j.molstruc.2016.11.084

[45] Öhström L. A short review of the terms 'Metal Organic Frameworks' The IUPAC project 'Coordination Polymers and Metal Organic Frameworks; Terminology and Nomenclature Guidelines [internet]. 2017. https://www.iupac.org/fileadmin/user_upload/databases/2009-012-2-200-short.review.pdf. [Accessed 2017-01-10] 2017.

[46] Freiser H, Morrison GH. Solvent extraction in radiochemical separations. Annual Review of Nuclear Science. 1959;**9**:221-255. DOI: 10.1146/annurev.ns.09.120159.001253

[47] Roig M, Kennedy JF, Macaskie LE. Biological rehabilitation of metal-bearing waste water. 1995. Final Report, EU Contract EV5V-CT93-0251. Brussels, The European Commission

[48] Davis Jr W. Solubilities of uranyl and iron (III) dibutyl and monobutyl phosphates in TBP solvent extraction systems. Contract No W-7405-eng 26 Oak Ridge National Laboratory, US Atomic Energy Commission[internet]. 1961. http://web.ornl.gov/info/reports/1961/3445600497148.pdf. [Accessed 29-01-2017]

[49] Rufus AL, Sathyaseelan VS, Narasimhan S, Velmurugan S. Dissolution of synthetic uranyl dibutyl phosphate deposits in oxidising and reducing chemical formulations. Journal of Hazardous Materials. 2013;**254-255**:263-269. DOI: 10.1016/j.jhazmat.2013.03.050

[50] Thomas RAP, Macaskie LE. Biodegradation of tributyl phosphate by naturally occurring microbial isolates and coupling to the removal of uranium from aqueous solution. Environmental Science and Technology. 1996;**30**:2371-2375. DOI: 10.1021/es9508611

[51] Owen S, Jeong BC, Poole PS, Macaskie LE. Tributyl phosphate degradation by immobilised cells of a *Citrobacter* sp. Applied Biotechnology and Biochemistry. 1992;**34**:693-707. DOI: 10.1007/BF02920590

[52] Thomas RAP, Macaskie LE. The effect of growth conditions on the biodegradation of tributyl phosphate and potential for the remediation of acid mine drainage waters by a naturally occurring mixed microbial culture. Applied Microbiology and Biotechnology. 1998;**49**:202-209

[53] Berne C, Montjarret B, Guountti Y, Garcia D. Tributyl phosphate degradation by *Serratia odorifera*. Biotechnology Letters. 2002;**26**:681-686. DOI: 10.1023/B:BILE.0000023030.69207.c0

[54] Berne C, Pignol D, Lavergre J, Garcia D. CYP201A2, a cytochrome p450 from *Rhodopseudomonas palustris*, plays a key role in the biodegradation of tributyl phosphate. Applied Microbiology and Biotechnology. 2007;**77**:135-144. DOI: 10.1007/s00253-007-1140-4

[55] Mennan C. Bacterial acid phosphatase and its application to waste remediation and metal recovery [PhD thesis]. University of Birmingham UK; 2011. http://etheses.bham.ac.uk/1017/1/Mennan11PhD1.pdf

[56] Tanaka N, Dumay V, Liao Q, Lange AJ, Wever R. Bromoperoxidase activity of vanadate-substituted acid phosphatases from *Shigella flexneri* and *Salmonella enterica* ser. Typhimurium. European Journal of Biochemistry 2002;**269**:2162-2167. DOI: 10.1046/j.1432-1033.2002.02871.x

[57] Michel LJ, Macaskie LE, Dean ACR. Cadmium accumulation by immobilized cells of *Citrobacter* sp. using various phosphate donors. Biotechnology and Bioengineering. 1986;**28**:1358-1365. DOI: 10.1002/bit.260280910

[58] Lugg H, Sannons RL, Marquis PM, Hewitt CJ, Paterson-Beedle M, Redwood MD, Stamboulis A, Kashani M, Jenkins M, Macaskie LE. Polyhydroxybutyrate accumulation by a *Serratia* sp. Biotechnology Letters. 2008;**30**:481-491. DOI: 10.1007/s10529-007-9561-9

[59] Wu CH, Lam BR, Chou J, Bill M, Brodie EL, Anderson GL, Hazen TC, Conrad ME, Henriksen J, Wright KE, Fujita Y. Microbial metabolism of triethylphosphate, a potential phosphate source for radionuclide mineralization processes. Eos Transactions American Geophysical Union Fall Meeting Supplement. 2009;**90**:H34A–08

[60] Bassil NM, Bryan N, Lloyd JR. Microbial degradation of isosaccharinic acid at high pH. International Society for Microbial Ecology Journal. 2014;**9**:310-320. DOI: 10.1038/ismej.2014.125

[61] Tian J, Yin J, Chi R, Rao G, Jiang M, Ouyang K. Kinetics on leaching rare earth from the weathered crust elution-deposited rare earth ores with ammonium sulfate solution. Hydrometallurgy. 2010;**101**:166-170. DOI: 10.1016/j.hydromet.2010.01.001

[62] Tian J, Yin J, Chi R, Rao G, Jiang M, Ouyang K. Optimisation of mass transfer in column elution of rare earths from low grade weathered crust elution-deposited rare earth ore. Hydrometallurgy. 2010;**103**:211-214. DOI: 10.1016/j.hydromet.2010.04.003

[63] Moldoveanu GA, Papangelakis VG. Recovery of rare earth elements adsorbed on clay minerals. II: leaching with ammonium sulfate. Hydrometallurgy. 2013;**131-132**:158-166. DOI: 10.1016/j.hydromet.2012.10.011

[64] Vavlekas D. Microbial recovery of rare earth elements from metallic wastes and scrap. [MRes Thesis]. University of Birmingham UK; 2016.

[65] Ohnuki T, Jiang M, Sakamoto F, Kozai N. Yamasaki S, Yu Q, Tanaka K, Utsunomiya S, Xia X, Yang K, He J. Sorption of trivalent cerium by a mixture of microbial cells and manganese oxides: Effect of microbial cells on the oxidation of trivalent cerium. Geochim et Cosmochim Acta. 2015;**163**:1-13. DOI: 10.1016/j.gca.2015.04.043

[66] Tobin KM, McGrath JW, Mullan A, Quinn J, O'Connor KE. Polyphosphate accumulation by *Pseudomonas putida* CA-3 and other medium chain length polyhydroxyalkanoate-accumulating bacteria under anaerobic growth conditions. Applied and Environmental Microbiology. 2007;**72**:1383-1387. DOI: 10.1128/AEM.02007-06

[67] Jiang M, Ohnuki T, Kozai N, Tanaka K, Suzuki Y, Sakamoto F, Kamiishi E, Utsunomiya S. Biological nano-mineralization of cerium phosphates by *Saccharomyces cerevisiae*. Chemical Geology. 2010;**277**:61-69. DOI: 10.1016/j.chemgeo.2010.07.010

[68] Dimović SD, Smičiklas ID, Šljivić-Ivanović MZ, Plećaš IB, Slavković-Beskoški L. The effect of process parameters on kinetics and mechanisms of Co^{2+} removal by bone char. Journal of Environmental Science and Health. A Toxic/Hazardous Substances and Environmental Engineering. 2011;**46**:1558-1569. DOI: 10.1080/10934529.2011.609454

[69] Anon. Guidance for the animal by-product industry. Department for Environment, Food and Rural Affairs, UK. 2014. https://www.gov.uk/government/collections/guidance-for-the-animal-by-product-industry. [Accessed 04-01-2017]

[70] Macaskie LE, Yong P, Thackray AC, Paterson-Beedle M, Marquis PM, Sammons RL, Nott KP, Hall LD. A novel non line of sight method for coating hydroxyapatite onto the surfaces of support materials by biomineralization. Journal of Biotechnology. 2005;**118**:187-200. DOI: 10.1016/j.jbiotec.2005.03.006

[71] Yong P, Paterson-Beedle M, Liu W, Zhang Z, Macaskie LE. A study of biofilm and non line of sight bio-hydroxyapatite coatings using a *Serratia* sp. Advanced Materials Research. 2009;**71-73**:741-744. DOI: 10.4028/www.scientific.net/AMR.71-73.741

[72] Holliday K, Handley-Sidhu S, Dardenne K, Renshaw J, Macaskie LE, Walther C, Stumpf T. A new incorporation mechanism for trivalent actinides into bioapatite: A TRLFS and EXAFS study. Langmuir. 2012;**28**:3845-3851. DOI: 10.1021/la300014a

[73] Handley-Sidhu S, Hriljac JA, Cuthbert MO, Renshaw JC, Pattrick RAD, Charnock JM, Stolpe B, Lead, JR, Macaskie LE. Bacterially-produced calcium phosphate nanobiominerals:

Sorption capacity, site preferences and stability of captured radionuclides. Environmental Science and Technology. 2014;**48**:6891-6898. DOI: 10.1021/es500734n

[74] Handley-Sidhu S, Renshaw JC, Yong P, Macaskie LE. Nanocrystalline hydroxyapatite biomineral for treatment of strontium from aqueous solutions. Biotechnology Letters. 2011;**33**:79-87. DOI: 10.1007/s10529-010-0391-9

[75] Handley-Sidhu S, Renshaw JC, Moriyama S, Stolpe B, Mennen C, Bagheriasi S, Yong P, Stamboulis A, Paterson-Beedle M, Sasaki K, Pattrick RAD, Lead JR, Macaskie LE. Uptake of Sr^{2+} and Co^{2+} into biogenic hydroxyapatite: Implications for biomineral ion exchange synthesis. Environmental Science and Technology. 2011;**45**:6985-6990. DOI: 10.1021/es2015132

[76] Bonthrone KM, Quarmby J, Hewitt CJ, Allan VJM, Paterson-Beedle M., Kennedy JF, Macaskie LE. The effect of the growth medium on the composition and metal binding behaviour of the extracellular polymeric material of a metal accumulating *Citrobacter* sp. Environmental Technology. 2000;**21**:123-134. DOI: 10.1080/09593330.2000.9618893

[77] Allan AJM, Callow ME, Macaskie LE. Effect of nutrient limitation on biofilm formation and phosphatase activity of a *Citrobacter* sp. Microbiology. 2002;**148**:277-288. DOI: 10.1099/00221287-148-1-277

[78] Gangappa R, Yong P, Singh S, Murray AJ, Macaskie LE. Hydroxyapatite biosynthesis by a *Serratia* sp and application of nanoscale bio-HA in the recovery of strontium and europium. Geomicrobiology Journal. 2016;**33**:267-273. DOI: 10.1080/01490451.2015.1067657

[79] Gangappa R, Farrier A, Macaskie LE. Eu^{3+} sequestration by biogenic nano-hydroxyapatite synthesized at neutral and alkaline pH. Geomicrobiology Journal. In press. DOI 10.1080/01490451.2016.1261966

[80] Beauregard D, Yong P, Macaskie LE, Johns ML. Using non-invasive magnetic resonance imaging to assess the reduction of Cr(VI) using a bio-palladium catalyst. Biotechnology and Bioengineering. 2010;**107**:11-20. DOI: 10.1002/bit.22791

[81] Wright KE, Hartmann T, Fujita Y. Inducing mineral precipitation in groundwater by addition of phosphate. Geochemical Transactions. 2011;**12**:8-20. DOI: 10.1186/1467-4866-12-8

[82] Van der Houwen JAM, Cressey G, Cressey BA, Valsami-Jones E. The effect of organic ligands on the crystallinity of calcium phosphate. Journal of Crystal Growth. 2003;**249**:572-583. DOI: 10.1016/S0022-0248(02)02227-3

[83] Thackray AC, Sammons RK, Macaskie LE. Yong P, Lugg H, Marquis PM. Bacterial synthesis of a calcium phosphate bon-substitute material. Journal of Materials Science Materials in Medicine. 2004;**15**,403-406. DOI: 10.1023/B:JMSM.0000021110.07796.6e

[84] Ledo HM, Thackray AC, Jones IP, Marquis PM. Macaskie LE, Sammons RL. Microstructure and composition of biosynthetically synthesised hydroxypatite. Journal of Materials Science Materials in Medicine. 2008;**19**:3419-3427. DOI: 10.1007/s10856-008-3485-3

[85] Terra J, Douado ER, Eon J-G, Ellis DE, Gonzalez G, Rossi AM. The structure of strontium-doped hydroxyapatite an experimental and theoretical study. Physical Chemistry Chemical Physics. 2009;**11**:568-577. DOI: 10.1039/b802841a

[86] Jensen J, Mackintosh AR. Rare earth magnetism. International Series Monographs in Physics. Birman J, Edwards SF, Llewellyn-Smyth CH, Rees M, editors. Oxford: Clarendon Press; 1991.http://www.fys.ku.dk/~jjensen/Book/Ebook.pdf [Accessed 2017-01-27]

[87] Schenk G, Ge Y, Carrington LE, Wynne CJ, Searle IR, Carroll BJ, Hamilton S, de Jersey J. Binuclear metal centers in plant purple acid phosphatises: Fe + Mn in sweet potato and Fe + Zn in soybean. Archives of Biochemistry and Biophysics. 1999;**370**:183-189. DOI: 10.1006/abbi.1999.1407

[88] Moriyama S, Mikheenko I, Macaskie LE. Magnetic Recovery of Neodymium in Bio-Hydroxyapatite. [Internet]. 2017.http://youtu.be/JIeC9nqeGpc [Accessed 2017-01-24]

[89] Singh, S. Use of *Serratia* sp. biofilm to recover rare earth element metals from model acidic waste solutions. [MSc Thesis] University of Birmingham UK; 2015.

[90] Murray AJ, Singh S, Vavlekas D, Tolley MR, Hathway TP, Boden R, Macaskie LE. A novel biomineralisation process for continuous selective recovery of rare earth elements. Proceedings of 53rd Annual Conference of Metallurgists, Vancouver Sept 28-Oct 1 2014 Paper 8669, 2014. Published by The Metallurgy & Materials Society of Canada, Quebec, Canada. ISBN: 978-1-926872-24-7

[91] Volesky B, editor. Biosorption of Heavy Metals. Boca Raton: CRC Press; 1990. p. 408

[92] Kotrba P, Mackova M, Macek T, editors. Microbial biosorption of metals. Dordrecht, Heidelberg, London, New York: Springer; 2011. p. 317. DOI: 10.1007/978-94-007-0443-5

[93] Paterson Beedle M, Readman JE, Hriljac JA, Macaskie LE. Biorecovery of uranium from aqueous solutions at the expense of phytic acid. Hydrometallurgy. 2010;**104**:524-528. DOI: 10.1016/j.hydromet.2010.01.019

[94] Mejare M, Bulow L. Metal-binding proteins and peptides in bioremediation and phytoremediation of heavy metals. Trends in Biotechnology. 2001;**19**:67-73. DOI: 10.1016/S0167-7799(00)01534-1

[95] Kuroda K, Ueda M. Engineering of microorganisms towards recovery of rare metal ions. Applied Microbiology and Biotechnology. 2010;**87**:53-60. DOI: 10.1007/s00253-010-2581-8

[96] Horiike T, Yamasjita M. A new fungal isolate, *Penidella* sp strain T9 accumulates the rare earth element dysprosium. Applied and Environmental Microbiology. 2015;**81**:3062-3086. DOI: 10.1128/AEM.00300-15